washed with water, dried ($MgSO_4$), and evaporated. The residue was redissolved in dichloromethane and flash chromatographed on silica gel (230-400 mesh, 5- × 25-cm). A band eluted first with 5% MeOH-CH_2Cl_2 solution. A second fraction was collected with 10-20% MeOH-CH_2Cl_2 solution. The product was eluted with 20-70% MeOH-CH_2Cl_2 solution. Partial evaporation of the solvent removed mainly dichloromethane to yield pure H_4(DPB) as purple microcrystalline powder (2.0 g, 23%). The ^{1}H NMR spectrum is the same as that reported in the literature.[24]

Co_2(DPB). In a dinitrogen drybox, a solution of 107 mg of free-base DPB, 364 mg of anhydrous cobalt(II) chloride, and 15 drops of 2,6-lutidine in 125 mL of THF was stirred and refluxed for 20 h. The resulting mixture was filtered through a column of neutral, activity I alumina (1- × 15-cm) to remove unreacted cobalt chloride. The solvent was removed under vacuum to yield Co_2(DPB) as a blood-red powder. Crystallization from dichloromethane/methanol yields analytically pure Co_2(DPB). Anal. Calcd for $C_{76}H_{76}N_8Co_2$: C, 74.86; H, 6.28; N, 9.19. Found: C, 74.83; H, 6.05; N, 9.04. Crystals for X-ray analysis were grown by slowly diffusing methanol into a chloroform solution of Co_2(DPB) at 5 °C. UV/vis (dichloromethane, nm): 382 (Soret), 530, 559 (lit.[10] 382, 530, 558 nm).

[Co_2(DPB)][PF_6]. In a dinitrogen drybox, 19.5 mg of Co_2(DPB) was dissolved in 15 mL of benzene with vigorous stirring. A THF solution of $AgPF_6$ (360 μL of a 4.31 × 10^{-2} M solution (21.8 mg in 2 mL of THF)) was added dropwise to the stirred solution. The mixture was stirred for 4 h after the final addition of oxidant. The reaction mixture was filtered through a glass-fiber plug in a pipette to remove precipitated silver metal and the oxidized product. The plug was washed with several milliliters of benzene to remove any unreacted starting material. The product was collected by washing the plug with dichloromethane until the washings remained colorless. Subsequent removal of the solvent under reduced pressure yielded 20.3 mg (93%) of [Co_2(DPB)][PF_6]. UV/vis (dichloromethane, nm): 372 (Soret), 524, 552 (lit.[10] 372 (Soret), 540 nm).

[(μ-O_2)Co_2(DPB)(DPIm)$_2$][PF_6]. 1,5-Diphenylimidazole (360 μL of an 8.33 × 10^{-2} M solution in dichloromethane) was added to a dioxygen-saturated solution of 20.3 mg of [Co_2(DPB)][PF_6]. The solvent was evaporated away under a stream of dioxygen. Recrystallization from chloroform/methanol yielded analytically pure [(μ-O_2)Co_2(DPB)(DPIm)$_2$][PF_6]. Anal. Calcd for $C_{106}H_{100}Co_2F_6N_{12}O_2P$: C, 69.31; H, 5.49; N, 9.15. Found: C, 69.43; H, 5.31; N, 9.08. UV/vis (dichloromethane, nm): 334, 410 (Soret), 534, 568. MS: LSIMS (tetraglyme) 1692 (cluster) [$M^+ - PF_6$].

Acknowledgment. We thank Kimoon Kim and Michele McMahon for contributions to the development of the improved synthesis of the free-base diporphyrin. We thank the National Science Foundation, the National Institutes of Health (Grants GM-17880 to J.P.C. and HL-13157 to J.A.I.), and the CNRS for financial support.

Supplementary Material Available: Table SI, additional bond distances and angles for Co_2(DPB), Table SII, final positional and thermal parameters for Co_2(DPB), and improved, large scale procedures for the preparation of compounds **8** and **9** (19 pages); Table SIII, structural amplitudes for Co_2(DPB) (31 pages). Ordering information is given on any current masthead page.

Synthesis and Characterization of Novel Cobalt Aluminum Cofacial Porphyrins. First Crystal and Molecular Structure of a Heterobimetallic Biphenylene Pillared Cofacial Diporphyrin

Roger Guilard,*[1a] Michel Angel Lopez,[1a] Alain Tabard,[1a] Philippe Richard,[1a] Claude Lecomte,[1b] Stéphane Brandes,[1a] James E. Hutchison,[1c] and James P. Collman[1c]

Contribution from the Laboratoire de Synthèse et d'Electrosynthèse Organométalliques, Associé au C.N.R.S. (URA 33), Faculté des Sciences "Gabriel", Université de Bourgogne (Dijon), 6, boulevard Gabriel, 21100 Dijon, France, Laboratoire de Minéralogie et Cristallographie, Associé au C.N.R.S. (URA 809), Université de Nancy I, B.P. 239, 54506 Vandoeuvre les Nancy, France, and Department of Chemistry, Stanford University, Stanford, California 94305.
Received April 8, 1992

Abstract: The synthesis of the novel family of heterodinuclear complexes (DP)CoAl(OR) (where DP^{4-} is the tetraanion of the diporphyrin biphenylene DPB or the diporphyrin anthracene DPA, and R = CH_3, CH_2CH_3, or $CH_2C_6H_5$) is reported. These complexes were obtained by selective metalation of the cofacial diporphyrins with cobalt and aluminum. Each (DP)CoAl(OR) complex was characterized by mass spectrometry and UV-vis, IR, ESR, and ^{1}H NMR spectroscopies. Unusually large paramagnetic shifts were observed for the protons on axial ligands bound to aluminum and for the porphyrinic N-H protons of the monocobalt DPB and DPA complexes. Analysis of the paramagnetic shifts indicates that the main contribution to isotropic shifts arises from a through space (or dipolar) interaction of an unpaired electron on cobalt(II). Structural data were deduced from the ^{1}H NMR study. In addition, the molecular structure of the cobalt(II) aluminum(III) ethoxide diporphyrin biphenylene (DPB)CoAl(OCH_2CH_3) was determined by X-ray diffraction. This is the first crystal structure of a heterobimetallic cofacial diporphyrin. (DPB)CoAl(OCH_2CH_3) ($C_{78}H_{81}N_8OCoAl\cdot C_7H_8$) crystallizes in the triclinic system, space group $P\bar{1}$. Its lattice constants are as follows: a = 13.095 (4) Å, b = 16.836 (3) Å, c = 16.986 (3) Å, α = 87.47 (1)°, β = 70.40 (3)°, γ = 85.90 (2)°, V = 3516 Å^3, Z = 2, $R(F)$ = 5.30%, $R_w(F)$ = 5.27%, GOF = 2.5 for 6800 reflections with $I \geq 3\sigma(I)$. No metal-metal interaction occurs (Co-Al = 4.370 (1) Å), and both porphyrin moieties are slipped by α = 29.8°. Finally, the tedious synthesis of the (DPA)H_4 free-base porphyrin has been extensively modified, and several new reaction steps are presented leading to significant increases in both scale and yield.

Many efforts of our groups have been devoted to the study of metalloporphyrins with metal-metal bonds[2-12] in order to investigate the major factors which affect the metal-metal interactions.[7,8,13] In these compounds most of metal-metal bonds

(1) (a) Université de Bourgogne (Dijon). (b) Université de Nancy I. (c) Stanford University.

(2) Barbe, J.-M.; Guilard, R.; Lecomte, C.; Gerardin, R. *Polyhedron* **1984**, *3*, 889-894.

0002-7863/92/1514-9877$03.00/0

characterized in dimeric metalloporphyrin complexes[3,5,7,8,13-22] exhibit diverse stabilities. Strong, multiple metal–metal bonds are well-established for the 4d and 5d metal centers but not for 3d metals. However, axial ligands weaken or destroy bonds between 4d and 5d metals. We have now synthesized new dimeric heterometalloporphyrins where the distances between the two macrocycles are fixed in an effort to form stable complexes. We have chosen two cofacial diporphyrins where the porphyrin rings are bridged via a rigid spacer group such as an anthracenyl ((DPA)H_4; DPA^{4-} = 1,8-bis[5-(2,8,13,17-tetraethyl-3,7,12,18-tetramethylporphyrinyl)]anthracene tetraanion) or a biphenylenyl ((DPB)H_4; DPB^{4-} = 1,8-bis[5-(2,8,13,17-tetraethyl-3,7,12,18-tetramethylporphyrinyl)]biphenylene tetraanion).[23-25] The geometries of these two cofacial diporphyrins are consistent with our initial target, which was the synthesis of mixed metal porphyrin dimers exhibiting a metal–metal interaction.

These face-to-face diporphyrins can also be efficient catalysts.[26-29] Of special interest is the synthesis of a mixed metal porphyrin dimer in which one porphyrin ring contains cobalt, an element known to bind dioxygen, and the other ring aluminum, an element that can serve as a Lewis acid.[30-33] Preliminary results indicate that the cobalt–aluminum complexes coordinate molecular oxygen via a reversible process.

In this paper we report the synthesis and the characterization of the novel family of heterodinuclear complexes (DP)CoAl(OR) (where DP^{4-} is the tetraanion of the diporphyrin biphenylene DPB or the diporphyrin anthracene DPA and R = CH_3, CH_2CH_3, or $CH_2C_6H_5$). These were obtained by selective metalation of the cofacial diporphyrins with cobalt and aluminum. In addition, the molecular structure of the cobalt(II) aluminum(III) ethoxide biphenylene diporphyrin (DPB)CoAl(OCH_2CH_3) was determined by X-ray diffraction. This is the first crystal structure of a heterobimetallic cofacial diporphyrin. Each (DP)CoAl(OR) complex has been characterized by mass spectrometry and UV–vis, IR, ESR, and ^1H NMR spectroscopies. The tedious synthesis of the (DPA)H_4 ligand[24] led us to modify and improve some steps in order to increase both the scale and the yield.

Experimental Section

Chemicals. The synthesis and handling of each heterobimetallic Co–Al complex was carried out under an argon atmosphere employing Schlenk techniques. Common solvents were dried in an appropriate manner and were distilled from the sodium benzophenone ketyl. Methylene chloride was dried over and distilled from CaH_2. Benzyl alcohol was distilled from sodium and stored over freshly activated 4-Å molecular sieves. Methanol and ethanol were dried over 3-Å and 4-Å molecular sieves, respectively, and degassed by bubbling for 30 min with argon. All other reagents were used as received. *N*-Bromosuccinimide (NBS) was recrystallized from water and thoroughly dried under high vacuum for several hours prior to use. Bis(tetrabutylammonium) dichromate (TBADC) was prepared from $K_2Cr_2O_7$ and Bu_4NBr as previously described.[34] Free-base diporphyrins (DP)H_4 were synthesized by some modifications of the literature procedures.[23-25]

Instrumentation. ^1H NMR spectra were recorded at 400 MHz on a Bruker WM400 spectrometer or at 200 MHz on a Bruker AC200 spectrometer of the C.S.M.U.B. (Centre de Spectrométrie Moléculaire de l'Université de Bourgogne) and all chemical shifts are reported relative to tetramethylsilane. Each solution contained between 3 and 5 mg of the complex. UV–vis spectra were recorded on a Perkin-Elmer 559 spectrometer or a Varian Cary 1 spectrometer. Infrared spectra were obtained on a Perkin-Elmer 580B apparatus. Solid samples were prepared as a 1% dispersion in CsI. ESR spectra were recorded in toluene at 100 K on a Bruker ESP300 spectrometer. Mass spectra were obtained with a Kratos Concept I S spectrometer in FABMS mode (primary atom beam, xenon; matrix, *m*-nitrobenzyl alcohol; accelerating voltage, 8 keV; ion current, 0.3 mA) or in DCIMS mode (gas: ammonia or isobutane). The data were collected and processed using a Sun 3/80 workstation.

Synthesis of (DPB)H_4 (1). The synthesis of (DPB)H_4 follows the procedure of Collman et al. described elsewhere.[35,36]

Synthesis of (DPA)H_4 (2). (DPA)H_4 has been prepared according to the following procedure.

1,8-Dichloroanthracene (3).[37] A 6-L reactor fitted with a mechanical stirrer and reflux condenser was charged with 1,8-dichloroanthraquinone (100 g, 0.36 mol) and aqueous ammonia (20%, 4 L). With stirring, zinc dust (400 g) and then cupric sulfate (1.7 g) were added over a few minutes. The red-brown mixture was gently heated for 90 min (large bubbles are formed). When the evolution of gas diminished, the temperature was raised to 80 °C and the suspension was stirred for 4.5 h. The hot mixture was filtered and gave a grey solid containing the product. The solid was thoroughly washed with water, partially dried by suction, and then stirred with three portions of acetone (3 × 800 mL). The combined acetone washes were evaporated to give an almost colorless solid. This material was dissolved in a minimum amount of hot 1-propanol (~600 mL) and HCl (11 M, ~2 mL) was added dropwise until

(3) Guilard, R.; Mitaine, P.; Moise, C.; Lecomte, C.; Boukhris, A.; Swistak, C.; Tabard, A.; Lacombe, D.; Cornillon, J.-L.; Kadish, K. M. *Inorg. Chem.* **1987**, *26*, 2467–2476.

(4) Guilard, R.; Lecomte, C.; Kadish, K. M. *Struct. Bonding* **1987**, *64*, 205–268.

(5) Guilard, R.; Zrineh, A.; Ferhat, M.; Tabard, A.; Mitaine, P.; Swistak, C.; Richard, P.; Lecomte, C.; Kadish, K. M. *Inorg. Chem.* **1988**, *27*, 697–705.

(6) Guilard, R.; Mitaine, P.; Moise, C.; Cocolios, P.; Kadish, K. M. *New J. Chem.* **1988**, *12*, 699–705.

(7) Guilard, R.; Kadish, K. M. *Comments Inorg. Chem.* **1988**, *7*, 287–305.

(8) Guilard, R.; Tabard, A.; Zrineh, A.; Ferhat, M. *J. Organomet. Chem.* **1990**, *389*, 315–324.

(9) Kadish, K. M.; Boisselier-Cocolios, B.; Swistak, C.; Barbe, J.-M.; Guilard, R. *Inorg. Chem.* **1986**, *25*, 121–122.

(10) Kadish, K. M.; Swistak, C.; Boisselier-Cocolios, B.; Barbe, J.-M.; Guilard, R. *Inorg. Chem.* **1986**, *25*, 4336–4343.

(11) Lecomte, C.; Habbou, A.; Mitaine, P.; Richard, P.; Guilard, R. *Acta Crystallogr., Sect. C: Cryst. Struct. Commun.* **1989**, *45*, 1226–1228.

(12) Loos, M.; Goulon, J.; Barbe, J.-M.; Guilard, R. *J. Phys.* **1986**, *47*(*C8*), 633–635.

(13) Guilard, R.; Zrineh, A.; Tabard, A.; Courthaudon, L.; Han, B. C.; Ferhat, M.; Kadish, K. M. *J. Organomet. Chem.* **1991**, *401*, 227–243.

(14) Boschi, T.; Licoccia, S.; Paolesse, R.; Tagliatesta, P. *Inorg. Chim. Acta* **1988**, *145*, 19–20.

(15) Cocolios, P.; Chang, D.; Vittori, O.; Guilard, R.; Moise, C.; Kadish, K. M. *J. Am. Chem. Soc.* **1984**, *106*, 5724–5726.

(16) Collman, J. P.; Barnes, C. E.; Collins, T. J.; Brothers, P. J. *J. Am. Chem. Soc.* **1981**, *103*, 7030–7032.

(17) Collman, J. P.; Brothers, P. J.; McElwee-White, L.; Rose, E.; Wright, L. J. *J. Am. Chem. Soc.* **1985**, *107*, 4570–4571.

(18) Collman, J. P.; Kim, K.; Garner, J. M. *J. Chem. Soc., Chem. Commun.* **1986**, 1711–1713.

(19) Del Rossi, K. J.; Wayland, B. B. *J. Am. Chem. Soc.* **1985**, *107*, 7941–7944.

(20) Onaka, S.; Kondo, Y.; Yamashita, M.; Tatematsu, Y.; Kato, Y.; Goto, M.; Ito, T. *Inorg. Chem.* **1985**, *24*, 1070–1076.

(21) Wayland, B. B.; Woods, B. A. *J. Chem. Soc., Chem. Commun.* **1981**, 475–476.

(22) Wayland, B. B.; Van Voorhes, S. L.; Wilker, C. *Inorg. Chem.* **1986**, *25*, 4039–4042.

(23) Chang, C. K.; Abdalmuhdi, I. *Angew. Chem., Int. Ed. Engl.* **1984**, *23*, 164–165.

(24) Chang, C. K.; Abdalmuhdi, I. *J. Org. Chem.* **1983**, *48*, 5388–5390.

(25) Eaton, S. S.; Eaton, G. R.; Chang, C. K. *J. Am. Chem. Soc.* **1985**, *107*, 3177–3184.

(26) Collman, J. P.; Hutchison, J. E.; Wagenknecht, P. S.; Lewis, N. S.; Lopez, M. A.; Guilard, R. *J. Am. Chem. Soc.* **1990**, *112*, 8206–8208.

(27) Ni, C.-L.; Abdalmuhdi, I.; Chang, C. K.; Anson, F. C. *J. Phys. Chem.* **1987**, *91*, 1158–1166.

(28) Liu, H.-Y.; Abdalmuhdi, I.; Chang, C. K.; Anson, F. C. *J. Phys. Chem.* **1985**, *89*, 665–670.

(29) Naruta, Y.; Maruyama, K. *J. Am. Chem. Soc.* **1991**, *113*, 3595–3596.

(30) Collman, J. P.; Kim, K.; Leidner, C. R. *Inorg. Chem.* **1987**, *26*, 1152–1157.

(31) Collman, J. P.; Bencosme, C. S.; Durand, R. R., Jr.; Kreh, R. P.; Anson, F. C. *J. Am. Chem. Soc.* **1983**, *105*, 2699–2703.

(32) Collman, J. P.; Hendricks, N. H.; Kim, K.; Bencosme, C. S. *J. Chem. Soc., Chem. Commun.* **1987**, 1537–1538.

(33) Ward, B.; Wang, C.-B.; Chang, C. K. *J. Am. Chem. Soc.* **1981**, *103*, 5236–5238.

(34) Santaniello, E.; Ferraboschi, P. *Synth. Commun.* **1980**, *10*, 75–81.

(35) (a) Collman, J. P.; Garner, J. M. *J. Am. Chem. Soc.* **1990**, *112*, 166–173. (b) Kim, K. Ph.D. Thesis, Stanford University, Stanford, CA, 1987.

(36) Collman, J. P.; Hutchison, J. E.; Lopez, M. A.; Tabard, A.; Guilard, R.; Seok, W. K.; Ibers, J. A.; L'Her, M. *J. Am. Chem. Soc.*, preceding paper in this issue.

(37) Golden, R.; Stock, L. M. *J. Am. Chem. Soc.* **1971**, *94*, 3080–3088.

crystals began to appear. Yellow needles rapidly formed. They were filtered off and washed with cold methanol to yield pure (**3**) (78.5 g, 88%). ^{1}H NMR (200 MHz ($CDCl_3$)): δ (ppm) 7.36 (dd, 2 H, J = 8.54 Hz, J = 7.20 Hz, 3,6-anth), 7.59 (d, 2 H, J = 7.20 Hz, 4,5-anth), 7.88 (d, 2 H, J = 8.54 Hz, 2,7-anth), 8.38 (s, 1 H, 10-anth), 9.18 (s, 1 H, 9-anth).

1,8-Dicyanoanthracene (4).[38,39] A 1-L three-necked round-bottomed flask fitted with a mechanical stirrer and reflux condenser was charged with 1,8-dichloroanthracene (**3**) (46.2 g, 0.19 mol), cuprous cyanide (74 g, 0.83 mol), and *N*-methylpyrrolidinone (freshly distilled over 4-Å molecular sieves, 500 mL). The mixture was refluxed under an inert atmosphere. The reaction was monitored by TLC (SiO_2, CH_2Cl_2: R_f(1,8-dichloroanthracene) = 0.80, R_f(1-chloro-8-cyanoanthracene) = 0.65, R_f(1,8-dicyanoanthracene) = 0.25). After 17 h, more cuprous cyanide was added. The reaction was nearly complete after an additional 50 h. The mixture was cooled (ice bath) and poured into 1 L of water with vigorous stirring. Aqueous ammonia (20%, 1 L) was then added, and the mixture was stirred for 4 days. The resulting brown precipitate was filtered and washed with water. The solid was again poured into aqueous ammonia (20%, 200 mL) and then filtered and washed with water. The residual cuprous cyanide was dissolved by treating the solid with 0.6 M aqueous sodium cyanide. The solid was filtered, washed with water, and then dried. Recrystallization with dimethylformamide (3 L) gave 29.18 g of pure 1,8-dicyanoanthracene (**4**) (68.4%). ^{1}H NMR (200 MHz ($CDCl_3$)): δ (ppm) 7.61 (dd, 2 H, J = 8.57 Hz, J = 6.89 Hz, 3,6-anth), 8.07 (d, 2 H, J = 6.89 Hz, 4,5-anth), 8.29 (d, 2 H, J = 8.57 Hz, 2,7-anth), 8.63 (s, 1 H, 10-anth), 9.14 (s, 1 H, 9-anth).

1,8-Diformylanthracene (5). A suspension of 1,8-dicyanoanthracene (**4**) (10 g, 43.85 mmol) in dry CH_2Cl_2 (freshly distilled under argon over CaH_2, 425 mL) was placed under argon in an ultrasonic cleaner for 10 min in order to dissolve most of the product. The suspension was then cooled to 0 °C with stirring. Diisobutylaluminum hydride (DIBAL-H, 88 mL, 1 M CH_2Cl_2 solution, 88 mmol) was rapidly added via a syringe. The reaction was monitored by TLC (SiO_2, CH_2Cl_2/heptane (5/1)). An additional 40 mL of DIBAL-H solution was added after 15 min. The yellow-brown mixture was stirred for 15 min at 0 °C and then for 30 min at room temperature. The solution was poured into aqueous sulfuric acid (50%, 350 mL) at 0 °C. At that stage, a large quantity of aluminum salts was formed. The mixture was diluted with water (4 L) in a separatory funnel, and the water layer was extracted with CH_2Cl_2 (4 times). The combined organic extracts were washed with water, dried over $MgSO_4$, and filtered. Most of the solvent was evaporated. Heptane was added to induce precipitation (−20 °C) of the product, which was recovered by filtration, washed with pentane, and dried under vacuum (8.33 g, 81%). ^{1}H NMR (200 MHz ($CDCl_3$)): δ (ppm) 7.70 (dd, 2 H, J = 4.22 Hz, J = 3.36 Hz, 3,6-anth), 8.13 (d, 2 H, J = 3.36 Hz, 4,5-anth), 8.30 (d, 2 H, J = 4.22 Hz, 2,7-anth), 8.60 (s, 1 H, 10-anth), 10.61 (s, 2 H, CHO), 11.19 (s, 1 H, 9-anth).

2-(Benzyloxycarbonyl)-3-ethyl-4-methylpyrrole (6). The preparation of **6** follows the literature procedure.[40-44] Instead of the ester pyrrole used in the initial published synthesis, the benzyl ester was synthesized because this compound is more easily converted to the corresponding carboxylic acid by hydrogenolysis.

1,8-Bis[5,5′-bis(benzyloxycarbonyl)-4,4′-diethyl-3,3′-dimethyl-2,2′-dipyrrylmethyl]anthracene (7). This derivative was prepared from **5** (5.64 g, 24 mmol) and **6** (23.3 g, 96 mmol) in the same manner as the biphenylene analogue,[35,36] and 26.9 g of **7** was obtained (95%). ^{1}H NMR (200 MHz ($CDCl_3$)): δ (ppm) 1.04 (t, 12 H, J = 7.36 Hz, CH_2CH_3), 1.56 (s, 12 H, CH_3), 2.69 (q, 8 H, J = 7.36 Hz, CH_2CH_3), 5.19 (s, 8 H, $CH_2C_6H_5$), 5.82 (s, 2 H, CH), 6.90 (d, 2 H, J = 7.23 Hz, 2,7-anth), 7.27 (br s, 20 H, $CH_2C_6H_5$), 7.36 (dd, 2 H, J = 7.23 Hz, J = 8.40 Hz, 3,6-anth), 7.97 (d, 2 H, J = 8.40 Hz, 4,5-anth), 8.29 (s, 1 H, 9-anth), 8.42 (br s, 4 H, NH), 8.51 (s, 1 H, 10-anth).

1,8-Bis(4,4′-diethyl-3,3′-dimethyl-2,2′-dipyrrylmethyl)anthracene (8). This compound was prepared from the tetraester **7** (25 g, 21.3 mmol) in the same manner as the biphenylene analogue[35,36] to yield 13.4 g (99%). ^{1}H NMR (200 MHz ($CDCl_3$)): δ (ppm) 1.19 (t, 12 H, J = 7.72 Hz, CH_2CH_3), 1.76 (s, 12 H, CH_3), 2.45 (q, 8 H, J = 7.72 Hz, CH_2CH_3), 5.99 (s, 2 H, CH), 6.32 (d, 4 H, J = 3.00 Hz, 5-pyrr), 7.04 (d, 2 H, J = 7.16 Hz, 2,7-anth), 7.30 (br s, 4 H, NH), 7.35 (dd, 2 H, J = 7.16 Hz, J = 7.88 Hz, 3,6-anth), 7.89 (d, 2 H, J = 7.88 Hz, 4,5-anth), 8.45 (s, 1 H, 9-anth), 8.69 (s, 1 H, 10-anth).

3,3′-Diethyl-5,5′-diformyl-4,4′-dimethyl-2,2′-dipyrrylmethane (9).[45] To a stirred solution of 3,3′-diethyl-4,4′-dimethyl-2,2′-dipyrrylmethane (34.5 g, 0.15 mol) in dry DMF (1 L) (freshly distilled under an inert atmosphere) cooled with an ice-water bath was added dropwise a solution of *p*-nitrobenzoyl chloride (85 g, 0.46 mol) in DMF (66 mL). A thick precipitate was formed after 5 min. The mixture was stirred at 0 °C for an additional 30 min and then allowed to warm to room temperature. Ether was added (1.6 L) and the mixture filtered. The solid product was washed with ether and then poured into 2.45 L of a 1.42 M solution of Na_2CO_3 in H_2O. The solution was gently heated for 20 min and then slowly cooled to 4 °C. After the solution was stored overnight in the refrigerator, the resulting orange precipitate was filtered, thoroughly washed with water, and dried under vacuum over NaOH (29.9 g, 69%). ^{1}H NMR (400 MHz ($CDCl_3$)): δ (ppm) 1.07 (t, 6 H, J = 7.55 Hz, CH_2CH_3), 2.29 (s, 6 H, CH_3), 2.46 (q, 4 H, J = 7.55 Hz, CH_2CH_3), 3.94 (s, 2 H, CH_2), 9.49 (s, 2 H, CHO), 10.65 (br s, 2 H, NH).

1,8-Bis[5-(2,8,13,17-tetraethyl-3,7,12,18-tetramethylporphyrinyl)]anthracene, (DPA)H_4 (2). This compound was synthesized from **8** (5.08 g, 8 mmol) and **9** (4.82 g, 16.8 mmol) by the same procedure used for (DPB)H_4.[35,36] Only the MeOH/CH_2Cl_2 ratios of the eluent during the flash chromatography were changed. The product was eluted as third fraction with 5–70% MeOH/CH_2Cl_2 solution to yield 1.64 g (18%). The ^{1}H NMR spectrum is identical to that reported in the literature.[24] IR (CsI): 3273 cm^{-1} (NH).

(DPB)ZnH_2. The synthesis of (DPB)ZnH_2 follows the procedure of Collman et al.[35] IR (CsI): 3286 cm^{-1} (NH).

(DPA)ZnH_2. The synthesis of (DPA)ZnH_2 follows the procedure of Collman et al.[35] for the DPB analogue. During the purification by column chromatography, the product band was eluted with 2–4% MeOH/CH_2Cl_2 solution (yield = 77%). IR (CsI): 3278 cm^{-1} (NH). DCIMS: m/z 1194 (cluster, $[M + H]^+$).

(DPB)CoH_2. To $(CH_3CO_2)_2Co{\cdot}4H_2O$ (550 mg, 2.2 mmol) and anhydrous sodium acetate (670 mg) dissolved in methanol (50 mL) was added a methylene chloride solution (600 mL) of (DPB)ZnH_2 (2.1 g, 1.79 mmol). After being stirred and refluxed for 4 h the mixture was cooled and washed with water (3 × 500 mL). Hydrochloric acid (6 M, 50 mL) was added, and the mixture was stirred vigorously for 30 min. The solution was neutralized with 10% sodium carbonate (130 mL), and the resulting mixture was vigorously stirred for 15 min. The organic phase was separated and washed sequentially with water and brine. The oxidized cobalt complex was reduced by heating the solution at reflux for 30 min in the presence of $NaBH_4$. The solution was washed again with water to neutralize the excess $NaBH_4$. The organic phase was separated, and methanol was added. After evaporation of CH_2Cl_2, the product was recovered by filtration as purple crystals (1.665 g, 80%). DCIMS: m/z 1163 (cluster, $[M + H]^+$). IR (CsI): 3284 cm^{-1} (NH).

(DPA)CoH_2. This compound was prepared from (DPA)ZnH_2 (800 mg) as described for its DPB analogue with the same yield. DCIMS: m/z 1189 (cluster, $[M + H]^+$). IR (CsI): 3279 cm^{-1} (NH).

(DPB)CoZn and (DPA)CoZn. These intermediate compounds were not isolated during the synthesis of the monocobalt diporphyrins. The metalation of (DP)CoH_2 (50 mg, 0.04 mmol) in CH_2Cl_2 (12 mL) with $(CH_3CO_2)Zn{\cdot}2H_2O$ (10 g/L methanolic solution, 1 mL, 0.05 mmol) followed by chromatographic purification (1- × 11-cm, SiO_2, CH_2Cl_2) quantitatively yielded the products. DCIMS: (DPB)CoZn m/z 1224 (cluster, $[M + H]^+$); (DPA)CoZn m/z 1251 (cluster, $[M + H]^+$).

(DP)Co(CH_3)Al(OR) (R = CH_3, CH_2CH_3, $CH_2C_6H_5$). The metalation procedure of Takeda and Inoue was used.[46,47] The synthesis was carried out in the dark due to the pronounced light sensitivity of σ-bonded complexes. At room temperature, trimethylaluminum (2 M solution in toluene, 0.25 mL) was slowly added via syringe to a stirred suspension of (DP)CoH_2 (250 mg, 0.215 mmol) in benzene (130 mL). The progress of the reaction was monitored by UV–vis spectroscopy. After 1 h the solvent was removed under reduced pressure. The purple residue was dissolved in methylene chloride, and insoluble material was filtered off. A large excess of alcohol (methanol, ethanol, or benzyl alcohol) was added to the red solution. The mixtures were heated under stirring at 50 °C during 20 h and then evaporated to dryness yielding quantitatively (DP)Co(CH_3)Al(OR) as a purple powder. DCIMS: (DPB)Co(CH_3)Al(OCH_3) m/z 1233 (cluster, $[M + H]^+$); (DPB)Co(CH_3)Al(OCH_2CH_3) m/z 1248 (cluster, $[M + H]^+$); (DPB)Co(CH_3)Al($OCH_2C_6H_5$) m/z 1310 (cluster, $[M + H]^+$); (DPA)Co(CH_3)Al(OCH_3) m/z 1260 (cluster,

(38) Akiyama, S.; Misumi, S.; Nakagawa, M. *J. Chem. Soc. Jpn.* **1960**, *33*, 1293–1298.
(39) Newman, M. S.; Boden, H. *J. Org. Chem.* **1961**, *26*, 2525.
(40) Badger, G. M.; Jones, R. A.; Laslett, R. L. *Aust. J. Chem.* **1964**, *17*, 1157–1163.
(41) Barton, D. H. R.; Zard, S. Z. *J. Chem. Soc., Chem. Commun.* **1985**, 1098–1100.
(42) Tindall, J. B. *Ind. Eng. Chem.* **1941**, *33*, 65–66.
(43) Sprang, C. A.; Degering, E. F. *J. Am. Chem. Soc.* **1942**, *64*, 1063–1064.
(44) Hartman, G. D.; Weinstock, L. M. *Org. Synth.* **1979**, *59*, 183–190.
(45) Chong, R.; Clezy, P. S.; Liepa, A. J.; Nichol, A. W. *Aust. J. Chem.* **1969**, *22*, 229–238.
(46) Inoue, S.; Takeda, N. *Bull. Chem. Soc. Jpn.* **1977**, *50*, 984–986.
(47) Takeda, N.; Inoue, S. *Bull. Chem. Soc. Jpn.* **1978**, *51*, 3564–3567.

Table I. X-ray Data for (DPB)CoAl(OEt)

formula	$C_{78}H_{81}N_8OCoAl \cdot C_7H_8$
fw, g mol^{-1}	1324.62
space group	triclinic $P\bar{1}$
cell dimensions	
a, Å	13.095 (4)
b, Å	16.836 (3)
c, Å	16.986 (3)
α, deg	87.47 (1)
β, deg	70.40 (3)
γ, deg	85.90 (2)
V, Å^3	3516
Z	2
$F(000)$, e$^-$	1406
d_{calc}, g cm^{-3}	1.251
μ, cm^{-1}	2.412
cryst dim, mm^3	0.30 × 0.16 × 0.32
radiation	Mo Kα; λ = 0.7107 Å
scan type	$\omega - 2\theta$
scan width, deg	1.0 + 0.34 tanθ
scan speed, deg min^{-1}	first set of data: 0.97–2.75 second set: 0.97
$(\sin\theta)/\lambda_{max}$, Å^{-1}	first set of data: 0.53 second set: 0.72
hkl	lower limit: 0, −22, −22 upper limit: 17, 22, 22
std reflections, exposure times	($0\bar{4}\bar{4}$, $3\bar{2}\bar{1}$, 104), 362 h
no. of reflcns measd	11 158
no. of unique reflcns ($I \geq 3\sigma(I)$)	6800
$R(F)$, %	5.3
$R_w(F)$, %	5.27
GOF	2.5

[M + H]$^+$); (DPA)Co(CH$_3$)Al(OCH$_2$CH$_3$) m/z 1274 (cluster, [M + H]$^+$); (DPA)Co(CH$_3$)Al(OCH$_2$C$_6$H$_5$) m/z 1336 (cluster, [M + H]$^+$).

(DP)CoAl(OR) (R = CH$_3$, CH$_2$CH$_3$, CH$_2$C$_6$H$_5$). In a Pyrex flask, the crude (DP)Co(CH$_3$)Al(OR) product was dissolved in benzene (150 mL). The solution was irradiated with a mercury lamp (OSRAM HQI-T400W/DV) for 40–60 h. ^{1}H NMR spectroscopy was used to determine completion of the reaction; then the benzene solution was evaporated to dryness. The DPB derivatives were recrystallized in a long glass tube by slow diffusion of heptane into a toluene solution of the compound at 4 °C. IR (CsI): (DPB)CoAl(OCH$_3$) 650 cm^{-1} (AlO); (DPB)CoAl(OCH$_2$CH$_3$) 642 cm^{-1} (AlO); (DPB)CoAl(OCH$_2$C$_6$H$_5$) 576 cm^{-1} (AlO); (DPA)CoAl(OCH$_3$) 660 cm^{-1} (AlO); (DPA)CoAl(OCH$_2$CH$_3$) 660 cm^{-1} (AlO); (DPA)CoAl(OCH$_2$C$_6$H$_5$) 583 cm^{-1} (AlO). DCIMS: (DPB)CoAl(OCH$_3$) m/z 1219 (cluster, [M + H]$^+$); (DPB)CoAl(OCH$_2$CH$_3$) m/z 1233 (cluster, [M + H]$^+$); (DPB)CoAl(OCH$_2$C$_6$H$_5$) m/z 1295 (cluster, [M + H]$^+$); (DPA)CoAl(OCH$_3$) m/z 1245 (cluster, [M + H]$^+$), (DPA)CoAl(OCH$_2$CH$_3$) m/z 1259 (cluster, [M + H]$^+$); (DPA)CoAl(OCH$_2$C$_6$H$_5$) m/z 1321 (cluster, [M + H]$^+$).

(DPB)Co(CH$_2$CH$_3$)Al(OCH$_3$). This compound was prepared according to the same procedure used for the (DPB)Co(CH$_3$)Al(OCH$_3$) analogue by using triethylaluminum instead of trimethylaluminum. DCIMS: m/z 1248 (cluster, [M + H]$^+$).

(DPB)[Al(OCH$_2$C$_6$H$_5$)]$_2$. To a stirred suspension of (DPB)H$_4$ (100 mg, 0.095 mmol) in benzene (50 mL) was added slowly triethylaluminum (1.9 M solution in toluene, 0.1 mL). The metalation reaction is rapid. After 15 min the solvent was evaporated to give (DPB)[Al(CH$_2$CH$_3$)]$_2$. ^{1}H NMR (400 MHz (C$_6$D$_6$)): δ (ppm) 9.33 (s, 2 H, H$_{meso}$), 8.71 (s, 4 H, H$_{meso}$), 6.97–6.75 (m, 6 H, biphen), 4.11 (m, 4 H, CH_2CH$_3$), 3.79 (m, 4 H, CH_2CH$_3$), 3.72 (m, 4 H, CH_2CH$_3$), 3.50 (m, 4 H, CH_2CH$_3$), 3.20 (m, 12 H, CH$_3$), 3.10 (m, 12 H, CH$_3$), 1.77 (t, 4 H, CH$_2$$CH_3$), 1.47 (t, 4 H, CH$_2$$CH_3$), −4.40 (t, 6 H, Al(CH$_2$$CH_3$)), −7.60 (q, 4 H, Al($CH_2CH_3$)).

The residue was dissolved in CH$_2$Cl$_2$ (20 mL) and filtered to remove insoluble material. Benzyl alcohol (10 mL) was added to the red solution, and the mixture was stirred at 50 °C for 15 h. Evaporation of the solution to dryness quantitatively yielded (DPB)[Al(OCH$_2$C$_6$H$_5$)]$_2$. ^{1}H NMR (400 MHz (C$_6$D$_6$)): δ (ppm) 9.19 (s, 2 H, H$_{meso}$), 8.72 (s, 4 H, H$_{meso}$), 6.95 (d, 2 H, biphen), 6.74 (t, 2 H, biphen), 6.51 (d, 2 H, biphen), 4.04 (m, 4 H, CH_2CH$_3$), 3.80 (m, 4 H, CH_2CH$_3$), 3.71 (m, 4 H, CH_2CH$_3$), 3.51 (m, 4 H, CH_2CH$_3$), 3.14 (m, 12 H, CH$_3$), 3.08 (m, 12 H, CH$_3$), 1.70 (t, 4 H, CH$_2$$CH_3$), 1.48 (t, 4 H, CH$_2$$CH_3$), 6.18 (dd, 2 H, H$_p$(Al(OCH$_2C_6H_5$))), 5.92 (dd, 4 H, H$_m$(Al(OCH$_2C_6H_5$))), 3.37 (d, 4 H, H$_o$(Al(OCH$_2C_6H_5$))), −1.42 (s, 4 H, Al(O$CH_2C_6H_5$)).

(OEP)Al(OCH$_2$C$_6$H$_5$). This compound was prepared from (OEP)H$_2$ (100 mg) and trimethylaluminum using the same procedure as for the DPB analogue (113 mg, 95%). ^{1}H NMR (400 MHz (C$_6$D$_6$)): δ (ppm) 10.35 (s, 4 H, H$_{meso}$), 3.97 (m, 16 H, CH_2CH$_3$), 1.85 (t, 24 H, CH$_2$$CH_3$), 6.51 (dd, 1 H, H$_p$(OCH$_2C_6H_5$)), 6.35 (dd, 2 H, H$_m$(OCH$_2C_6H_5$)), 4.34 (d, 2 H, H$_o$(OCH$_2C_6H_5$)), −0.08 (s, 2 H, O$CH_2C_6H_5$).

Scheme I

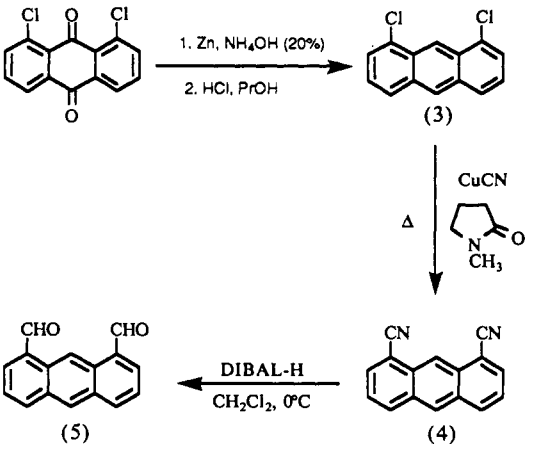

Crystal and Molecular Structure of (DPB)CoAl(OCH$_2$CH$_3$). After many unsuccessful crystallization tests, suitable crystals were obtained as follows. The title compound was recrystallized in a 7-mm diameter, 20-cm-long glass tube by slow diffusion of heptane into a toluene solution of the compound (35 mg in 1 mL). Crystals were allowed to grow for 1 month at 4 °C. From the batch of crystals obtained a 0.30 × 0.16 × 0.32 mm^3 crystal was selected. Preliminary oscillation and Weissenberg photographs showed a triclinic cell whose constants are given in Table I. Cell parameters and intensity data were measured on an Enraf–Nonius CAD4F diffractometer at room temperature, with graphite monochromatized Mo Kα radiation in the following way. First all the data in half a sphere of radius 0.53 Å^{-1}, $(\sin\theta)/\lambda$ were collected. These data were used for the preliminary crystal structure solution. The approximate fractional coordinates of the atoms and their isotropic thermal parameters then enabled us to calculate the intensities of higher order reflections, and intensities in the range of 0.53–0.72 Å^{-1}, $(\sin\theta)/\lambda$ which were estimated to have $I \geq 3\sigma(I)$ were measured on the same crystal specimen at constant scan speed (Table I). All the data were reduced with the SDP data reduction programs;[48] a monotonic linear decay of 3.1% calculated from the three $0\bar{4}\bar{4}$, $3\bar{2}\bar{1}$, and 104 standard reflections was then applied to the whole data set; no absorption and beam inhomogeneity correction was deemed necessary. The structure was solved in the centrosymmetric group $P\bar{1}$ by direct methods (MULTAN82)[48] and subsequent Fourier syntheses. All non-hydrogen atoms of the molecule were located, as well as a toluene solvate molecule; this latter solvent molecule was refined as a rigid group with the SHELX 76 program.[49] Hydrogen atoms were then included in the structure factor calculations either at their calculated positions for the atoms attached to ethyl and trigonal carbon atoms or as located in Fourier difference maps for those attached to methyl carbon atoms. After several cycles of anisotropic least-squares refinement in two blocks (Block 1: scale factor, xyz, and U^{ij} of the Co porphyrin + biphenylene connector. Block 2: xyz and U^{ij} of the aluminum porphyrin + toluene solvate.), a Fourier difference map revealed that the ethoxide ligand linked to the aluminum atom was disordered. This disorder was modeled by allowing two positions of this group, whose occupancies were refined to be 0.76 (6) and 0.24 (6). At the end of the refinement the statistical indices of fit were $R(F)$ = 5.30%, $R_w(F)$ = 5.27%, and GOF = 2.5. The rather high value of the goodness of fit shows that the model used for the disordered ethoxide group is not entirely satisfactory, but other attempts at modeling did not lead to better and more chemically reasonable results. Table II gives the main distances and angles of the molecule. Tables of anisotropic thermal motion parameters, a table of full bond distances and angles, least-squares planes, positional parameters for hydrogen atoms, positional parameters and estimated standard deviations, a list of structure factors, and an ORTEP drawing of the molecule are available as supplementary materials.

Results and Discussion

Synthesis of (DPA)H$_4$. The synthesis of this diporphyrin is long because its convergent synthesis involves three major branches.

(48) *SDP: Structure Determination Package*; Enraf-Nonius: Delft, The Netherlands, 1977.

(49) Sheldrick, G. M. *SHELX 76: Program for Crystal Structure Determinations*; University of Göttingen: Göttingen, Fed. Rep. Ger., 1976.

Scheme II

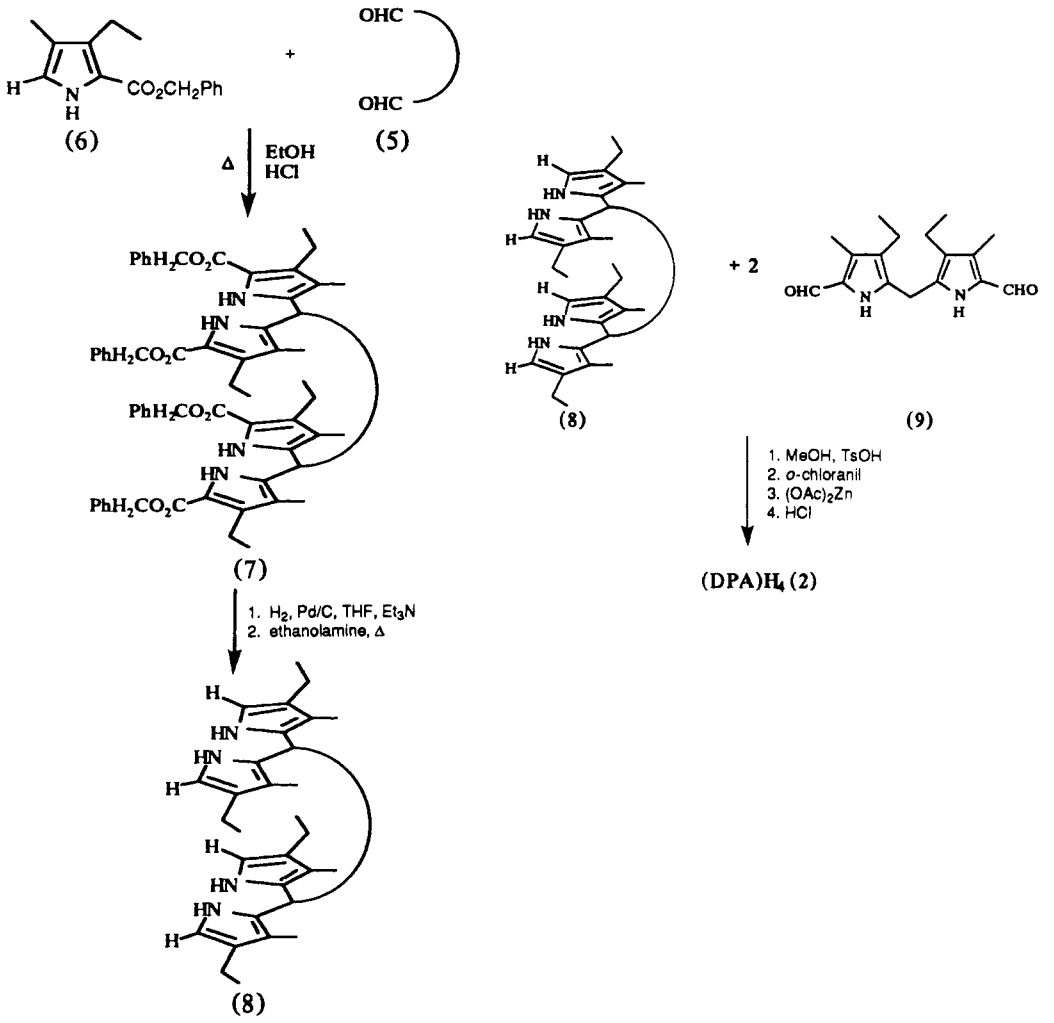

Scheme III

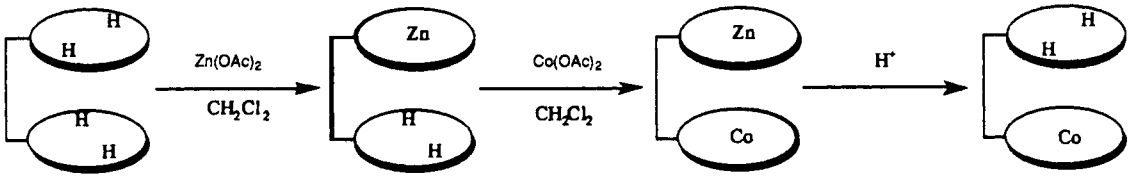

In the first branch the anthracenyl bridge (Scheme I) which joins the two porphyrin rings is constructed.

The porphyrin macrocycle of the cofacial diporphyrins is composed of the products of the other two branches. The second branch leads to the trisubstituted pyrrole **6**, while the third branch gives the dialdehyde **9**. Condensation of these intermediates leads to the free-base cofacial diporphyrin (Scheme II).

We describe a significant modification in the synthesis of the anthracenedicarbaldehyde **5**. For the synthesis of this compound, Chang refers to a paper[24] describing the preparation of **5** from 1,8-dicyanoanthracene (**4**) through a long series of reactions including hydrolysis, esterification, reduction to the alcohol, and then oxidation. We discovered that **5** can be prepared from **4** in high yield via a single step involving treatment of **4** with diisobutylaluminum hydride (DIBAL-H), followed by acid hydrolysis (Scheme I). The condensation reaction of a solution of bis(dipyrrylmethane) **8** with dicarboxaldehyde dipyrrylmethane **9** (Scheme II) was carried out in presence of *p*-toluenesulfonic acid in the dark. The zinc diporphyrin was easily isolated from the reaction mixture by a silica column chromatography. The free base was then regenerated with dilute hydrochloric acid and purified by flash chromatography. Several changes in reaction conditions were tested, and the highest observed yield was 18% for $(DPA)H_4$ compared to the 7% yield reported in the original preparation.[24] The use of *p*-toluenesulfonic acid as catalyst and long reaction times (48 h) are crucial. The yield is strongly dependent on the addition time and purity of *p*-toluenesulfonic acid. The modifications and improvements of the original synthetic scheme for the synthesis of anthracene-bridged cofacial diporphyrins allowed us to scale up each step and prepare large quantities of this cofacial diporphyrin.

Synthesis of (DP)CoAl(OR) (DP = DPB or DPA and R = CH_3, CH_2CH_3, or $CH_2C_6H_5$). A synthesis of the monocobalt complex $(DPA)CoH_2$ has been reported; however, the product was only characterized on the basis of mass spectral data.

Attempts to insert cobalt into the free base were unsuccessful in producing high yields of the monometalated product, so another approach was investigated. We have synthesized the $(DP)CoH_2$ complexes according to Scheme III. One porphyrin is protected by metalation with Zn(II) to yield the $(DP)ZnH_2$ complex.[35] The free-base porphyrin of this complex can then be metalated with $Co(OAc)_2$ to yield the Co–Zn complex. Treatment with $NaBH_4$ and then demetalation of the zinc porphyrin but not the cobalt porphyrin led to the monocobalt(II) porphyrin.

The (DP)CoAl(OR) heterobinuclear complexes were obtained according to Scheme IV. Metalation of $(DP)CoH_2$ complexes

Scheme IV

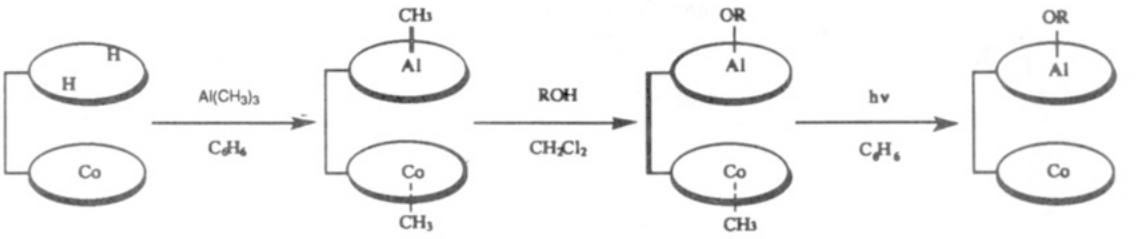

Table II. Selected Bond Distances (Å) and Angles (deg) for (DPB)CoAl(OEt)[a]

Co–Al	4.370 (1)	Al–O1	1.789 (3)
Co–N1	1.963 (4)	Al–N1*	2.005 (4)
Co–N2	1.952 (3)	Al–N2*	2.003 (3)
Co–N3	1.952 (4)	Al–N3*	2.005 (4)
Co–N4	1.958 (3)	Al–N4*	1.996 (3)
N1–Co–N2	88.9 (1)	N1*–Al–N2*	86.8 (1)
N1–Co–N4	91.4 (1)	N1*–Al–N4*	89.4 (1)
N2–Co–N3	91.3 (1)	N2*–Al–N3*	89.3 (1)
N3–Co–N4	88.9 (1)	N3*–Al–N4*	87.1 (1)
O1–Al–N1*	99.1 (2)		
O1–Al–N3*	98.0 (1)		
O1–Al–N2*	103.9 (1)		
O1–Al–N4*	101.2 (1)		

bond type[b]	mean[c]	angle type[b]	mean[c]
N–Ca	1.382 (7)	Ca–N–Ca	104.8 (7)
Ca–Cb	1.444 (11)	N–Ca–Cb	110.6 (6)
Cb–Cb	1.347 (8)	N–Ca–Cm	124.2 (7)
Ca–Cm	1.374 (10)	Ca–Cb–Cb	106.9 (5)
Cb–Cm1	1.505 (9)	Cb–Cb–Cm1	123.5 (4)
Cb–Cm2	1.505 (9)	Cb–Cb–Cm2	127.9 (8)
Cb–Ce1	1.500 (8)	Ca–Cb–Cm1	129.7 (4)
Ce1–Ce2	1.518 (12)	Ca–Cb–Cm2	124.8 (5)
		Cb–Cb–Ce1	128.0 (5)
		Ca–Cb–Ce1	125.0 (6)
		Cb–Ce1–Ce2	112.3 (7)

[a] See Figure 1 for atom-labeling scheme. [b] Average of equivalent bonds and angles of the porphyrin rings. For steric reasons, the methyl groups close to the biphenylene connector are different from the others and are distinguished. The atoms are labeled as follows:

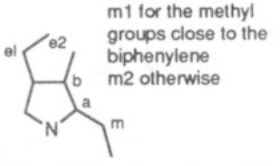

[c] The standard deviations of the mean values $\sigma(\bar{d})$ are the larger of the esd of a single observation and of

$$\sigma_{\text{calcd}}(\text{d}) = \left[\frac{N}{(N-1)}[(\overline{d^2}) - \bar{\text{d}}^2]\right]^{1/2}$$

for N equivalent bonds.

with $Al(CH_3)_3$ gives the cobalt–aluminum (DP)Co(CH_3)Al(CH_3) complexes in which the two metals each have an axial methyl group.

In presence of alcohol, the methyl ligand of the Al atom is substituted by an alkoxide group. Photolysis of this complex induces the reductive cleavage of the Co^{III}–CH_3 bond leading to the (DP)CoAl(OR) derivatives.

Crystal Structure of (DPB)CoAl(OCH_2CH_3). The present paper describes the first heterobimetallic "Pacman" porphyrin; preliminary results of the structure have been reported.[50] Figure 1 shows the molecular structure of (DPB)CoAl(OEt) (a, b) and the atomic numbering scheme used (c). The only published crystal structures of the Pacman porphyrins are (DPB)Co_2,[36] (DPB)Cu_2,[51] and (DPA)Ni_2.[51] The porphyrin groups of these latter molecules are slipped with respect to each other, leading to metal–metal distances equal to 3.726, 3.807, and 4.566 Å, respectively. The porphyrin rings of (DPB)CoAl(OEt) are also slipped. The Co–Al

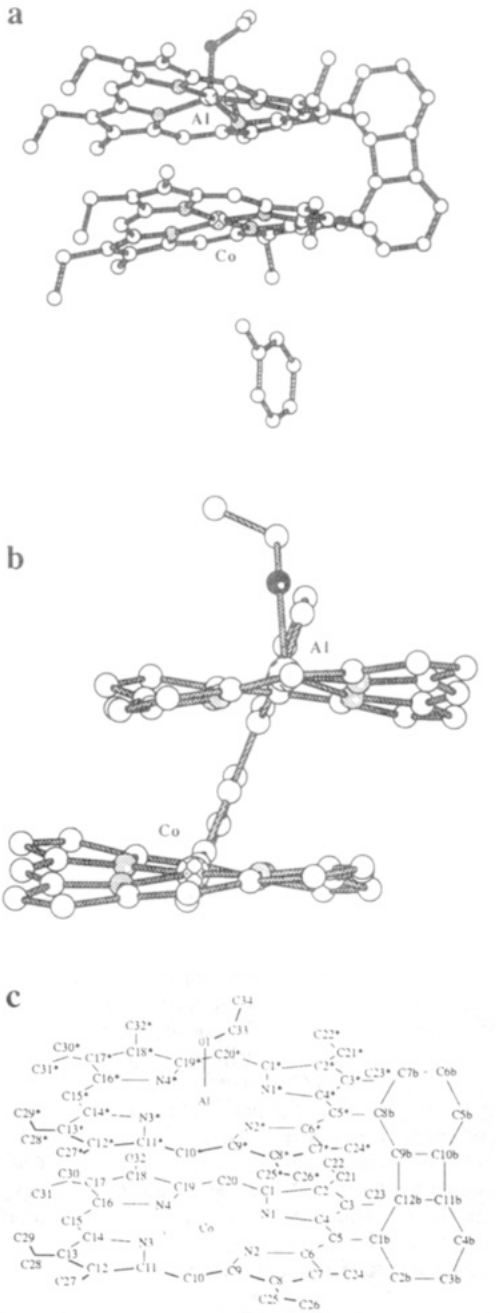

Figure 1. Molecular structure of (DPB)CoAl(OCH_2CH_3): (a) X-ray crystal structure of the whole molecule plus the toluene solvate, (b) same molecule in a different orientation, excluding side groups, and (c) numbering scheme used.

(50) Richard, P.; Lopez, M. A.; Guilard, R.; Lecomte, C.; Hutchison, J.; Collman, J. P. *XVth Congress of International Union of Crystallography*, Bordeaux, France, 1990.

(51) Fillers, J. P.; Ravichandran, K. G.; Abdalmuhdi, I.; Tulinsky, A.; Chang, C. K. *J. Am. Chem. Soc.* **1986**, *108*, 417–424.

Table III. Comparison of the Conformational Parameters for the Biphenylene Cofacial Metalloporphyrins (See Text for the Meaning of the Different Parameters)

compound	Ct_1–Ct_2 (Å)	tilt (deg)	α (deg)	Sr (Å)	Sp (Å)	ref
(DPB)Cu_2	3.86	4.4	25.0	3.50	1.63	51
(DPB)CuMnCl	3.94	5.2	25.8	3.54	1.71	55
(DPB)CoAl(OEt)	4.08	7.4	29.8	3.54	2.03	this work

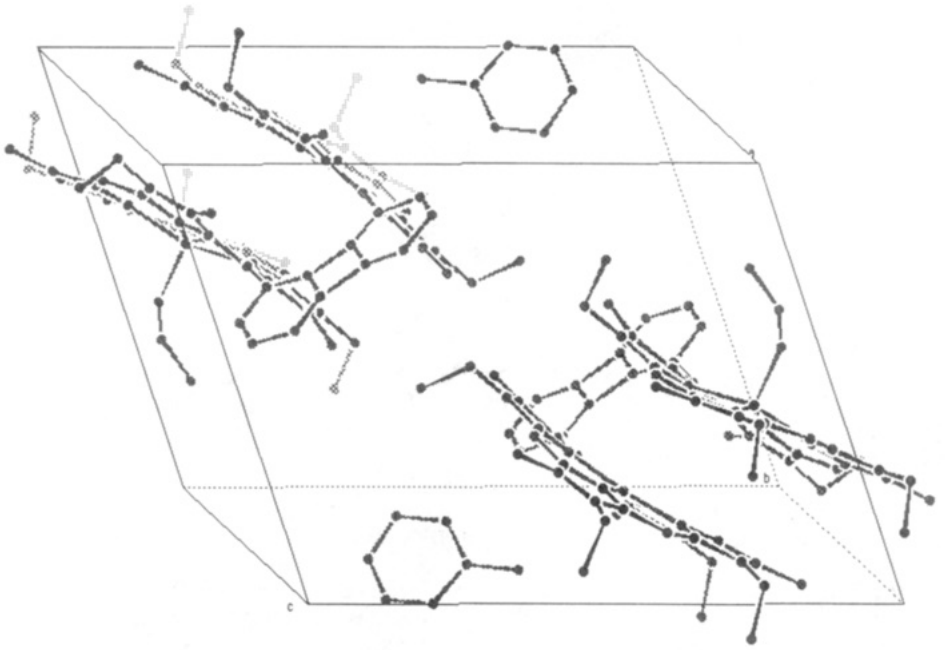

Figure 2. View of the unit cell for (DPB)CoAl(OCH_2CH_3)·(C_7H_8).

Scheme V

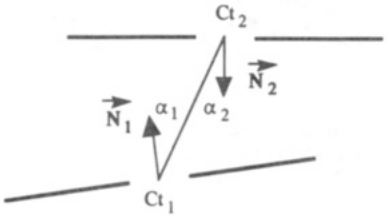

distance is 4.370 (1) Å; hence no metal–metal interaction occurs. The cobalt atom is four coordinate. The average Co–N distance is 1.956 (5) Å (1.949 (1) Å in (TPP)Co).[52] The aluminum atom is five coordinate, and the axial ethoxide ligand is located outside the cavity. The aluminum atom lies 0.365 (1) Å from the four-nitrogen plane in the direction of the ethoxide ligand. The Al–O distance is 1.789 (3) Å; the average Al–N distance is 2.002 (4) Å, and this value compares very well with that found in (OEP)Al(CH_3) (⟨Al–N⟩ = 2.033 (3) Å).[53] The two macrocycles are not parallel, and their mean least-squares planes are tilted by 7.4°. Therefore, for such a molecule, we can define a set of conformation parameters which are as follows (Scheme V). If $\mathbf{N}_i$ (i = 1, 2) is the unit vector normal to the 24-atom average plane and $\mathbf{Ct_1Ct_2}$ is the vector joining the two 4-nitrogen centers, then

$$\cos(\alpha_i) = \frac{\mathbf{N}_i \cdot \mathbf{Ct_1Ct_2}}{|\mathbf{Ct_1Ct_2}|}$$

The slip angle α is calculated as the average of α_1 and α_2, the slip parameter being Sp = $|\mathbf{Ct_1Ct_2}|\cdot\sin(\alpha)$. The inter-ring separation is defined by Sr = $|\mathbf{Ct_1Ct_2}|\cdot\cos(\alpha)$.[54] Table III gives the α, Sp, Sr, and some other conformational values of (DPB)CoAl(OEt) compared to those of (DPB)Cu_2[51] and (DPB)CuMnCl.[55] As shown in this table, the slipped conformation is the main characteristic of this class of compounds. The inter-ring separation is the same for the three compounds, and their slip parameters varies from 1.63 Å in (DPB)Cu_2[51] to 2.03 Å in (DPB)CoAl(OEt). It is related to the usual interaction between π molecular systems. It is well-known that porphyrins in crystals often adopt such a stacked geometry with their centers offset.[56] Recently Sanders and Hunter[57] developed a simple electrostatic model of the charge distribution in a π-system which can be applied to this observed geometry. Their model considers the σ- and the π-electron systems separately and shows that the bonding interaction is mainly due to π–σ electrostatic interactions that overcome π–π repulsion. The geometrical requirement for such bonding interaction imposes an offset of the two centers of the stacked aromatic molecules. This model was applied to various systems like porphyrin–porphyrin, porphyrin–solvent, and other aromatic–aromatic molecules with π interactions. The experimental results are in agreement with such a model. This interpretation explains the slipped geometry observed in this class of Pacman porphyrins. Nevertheless other factors can break this electrostatic constraint: our preliminary X-ray crystal structures of the (DPB)CoCu and (DPB)Zn_2 complexes obtained from a slow electrochemical oxidation process show that the two porphyrin groups are not slipped but face-to-face in an eclipsed cofacial geometry.[58] In this case, the partial oxidation of the π-system could induce a clear π–π bonding interaction; the largest would be the π–π overlap between the two systems. This is, of course, achieved with an eclipsed conformation and not for a slipped one.[59,60]

(52) Stevens, E. D. *J. Am. Chem. Soc.* **1981**, *103*, 5087–5095.
(53) Guilard, R.; Zrineh, A.; Tabard, A.; Endo, A.; Han, B. C.; Lecomte, C.; Souhassou, M.; Habbou, A.; Ferhat, M.; Kadish, K. M. *Inorg. Chem.* **1990**, *29*, 4476–4482.
(54) The inter-ring separation could also be defined as the average of the closest contact distances between pairs of atoms belonging to the two rings; this led to an inter-ring separation of 3.65 (13) Å for (DPB)CoAl(OEt).
(55) Guilard, R.; Brandes, S.; Tabard, A.; Bouhmaida, N. D.; Lecomte, C.; Richard, P.; Collman, J. P. Manuscript in preparation.
(56) Scheidt, W. R.; Lee, Y. J. *Struct. Bonding* **1987**, *64*, 1–70.
(57) Hunter, C. A.; Sanders, J. K. M. *J. Am. Chem. Soc.* **1990**, *112*, 5525–5534.
(58) Guilard, R.; Barbe, J.-M.; Richard, P.; Gindrey, V.; Lecomte, C. Unpublished results.

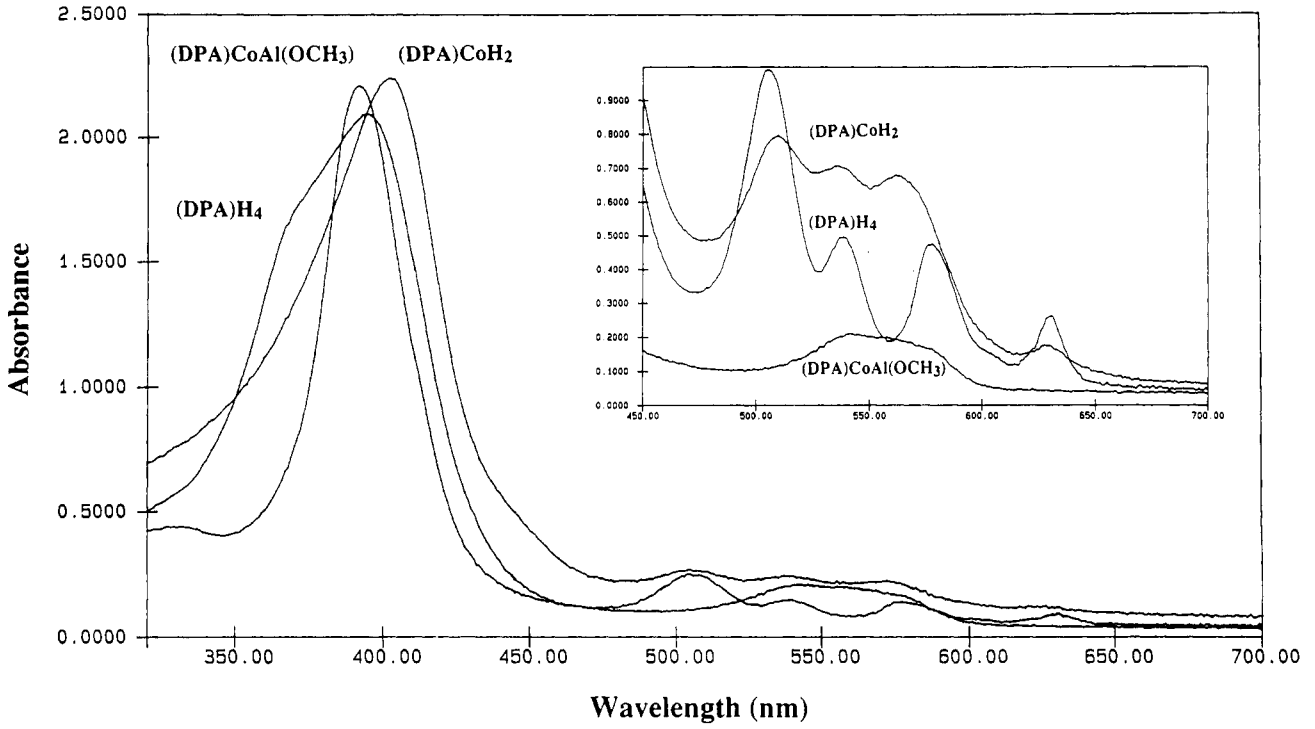

Figure 3. Comparison of UV–vis spectra of $(DPA)H_4$, $(DPA)CoH_2$, and $(DPA)CoAl(OCH_3)$ recorded in benzene.

Another characteristic of this molecule which is common to the $(DPB)Cu_2$, $(DPB)Co_2$,[36] and (DPB)CuMnCl[55] complexes is the severe nonplanarity of the porphyrin rings: the average deviations of the atoms from the two mean porphyrin planes are the same (0.22 Å) with a maximum value of 0.51 Å. The pyrrole rings are alternatively tilted above and below the mean porphyrin plane.

The biphenylene connector compares quantitatively with the biphenylene structure.[61] The average deviations of the atoms from the mean biphenylene plane is 0.027 Å with a maximum value of 0.055 (5) Å. The dihedral angles between the biphenylene mean plane and the two porphyrin mean planes are 20.91 (4)° and 23.12 (4)°, respectively. All bond distances and angles of the porphyrin ring are in excellent agreement with those reported for (TPP)Co[52] and $(OEP)Al(CH_3)$.[53]

The triclinic $P\bar{1}$ unit cell contains two diporphyrin molecules and two toluene solvates which are related by the inversion center as shown in Figure 2. The orientation of the solvate molecule is not usual; in most solvated porphyrin crystal structures the solvate (toluene or benzene molecule) is almost parallel to the porphyrin moiety in order to increase the π–π interactions.[57] In the present crystal structure the toluene molecules are almost perpendicular to the porphyrin plane and the closest contact is 3.510 (6) Å between the toluene molecule and a methyl carbon atom of the cobalt porphyrin (C300–C24) (see supplementary material).

The DPA and DPB complexes have been characterized by mass spectrometry and IR, UV–vis, ^1H NMR, and ESR spectroscopy.

Mass Spectrometry. The mass spectral data are given in the Experimental Section. The molecular peak of the diporphyrin complexes is observed for each derivative, and these data agree well with the expected molecular formula. The fragmentation pattern is strongly dependent on the coordination scheme of the metal centers. For the four-coordinate complexes, i.e., the derivatives containing the cobalt(II) and zinc(II) ions, the molecular peak is the parent peak. For the aluminum(III)–cobalt(III) complexes where the metal centers are five coordinate, the parent peak fits either the fragment $[M - R_1]^+$ ($(DP)Co(R_1)Al(OR)$) or $[M - R_1 - R_2]^{\bullet+}$ ($(DP)Co(R_1)Al(R_2)$). These fragmentation patterns are in good agreement with those observed for other σ-bonded alkyl (or aryl) complexes in metalloporphyrin chemistry.[4,62–65] For the alkoxide aluminum derivatives, the $[(DP)CoAl]^+$ fragment corresponding to the loss of the alkoxide group is observed with a lower intensity than that of the $[(DP)CoAl(OR)]^{\bullet+}$ fragment. These results can be explained by the relative lability of the different axial bonds, i.e., the σ metal–carbon bond versus the metal–alkoxide bond.

Infrared Spectroscopy. The monometallic complexes exhibit a characteristic vibrational band in the range of 3278–3286 cm^{-1} which is due to the N–H stretching mode of the metal-free porphyrin pyrrole NH groups.[66] Although we do not observe any shift in ν(NH) upon monometalation of a cofacial diporphyrin, the intensity of this band is reduced for these monometallic derivatives. The ultimate bimetallic derivatives (DP)CoAl(OR) show a characteristic vibrational band ν(Al–O) in the range of 576–660 cm^{-1} (see Experimental Section), and these data agree well with those reported for other aluminum alkoxide complexes.[67] As expected, the decreased frequency depends on the nature of the aluminum axial ligand according to the sequence $\nu(AlOCH_3) > \nu(AlOCH_2CH_3) > \nu(AlOCH_2C_6H_5)$. These data are in accordance with the highest value observed for (DPB)CoAl(OH) (ν(AlOH) = 691 cm^{-1}). In contrast, the cobalt oxidation state appears to have no effect.

UV–Vis Spectroscopy. The UV–vis data for the Pacman free-base porphyrins and their corresponding mono- and bimetallic

(59) For this kind of compound the only two possible conformations are the slipped one and the eclipsed one; the staggered conformation is not allowed due to the rigid pillar connector. However, for the HOMO A_{2u} π orbitals the maximal overlap is achieved for a rotation angle $\phi = 0°$. In contrast, partially oxidized phthalocyanine material presents a staggered conformation due to the largest overlap of the HOMO A_{1u} π orbitals for a rotation angle $\phi = 0$ or 45°.

(60) Newcomb, T. P.; Godfrey, M. R.; Hoffman, B. M.; Ibers, J. A. *Inorg. Chem.* **1990**, *29*, 223–228.

(61) Fawcett, J. K.; Trotter, J. *Acta Crystallogr.* **1966**, *20*, 87–93.

(62) Kadish, K. M.; Boisselier-Cocolios, B.; Cocolios, P.; Guilard, R. *Inorg. Chem.* **1985**, *24*, 2139–2147.

(63) Kadish, K. M.; Boisselier-Cocolios, B.; Coutsolelos, A.; Mitaine, P.; Guilard, R. *Inorg. Chem.* **1985**, *24*, 4521–4528.

(64) Tabard, A.; Guilard, R.; Kadish, K. M. *Inorg. Chem.* **1986**, *25*, 4277–4285.

(65) Guilard, R.; Kadish, K. M. *Chem. Rev.* **1988**, *88*, 1121–1146.

(66) Alben, J. O. In *The Porphyrins*; Dolphin, D., Ed.; Academic: New York, 1978; pp 323–345.

(67) Malowsky, E., Jr. *Vibrational Spectra of Organometallic Compounds*, 1st ed.; Wiley Interscience: New York, 1977; pp 1–528.

Table IV. UV–Vis Data for the $(DPB)H_4$ and $(DPA)H_4$ Free-Base Porphyrins and Their Corresponding Metalated Derivatives in Benzene

compound	λ_{max}, nm ($\epsilon = 10^{-3}$ M^{-1} cm^{-1})				
	Soret region	Q bands			
$(DPB)H_4$	379 (173.9)	511 (6.3)	540 (2.0)	580 (3.4)	632 (1.8)
$(DPB)ZnH_2$	388 (200.0)	518 (4.1)	542 (5.2)	581 (6.8)	633 (0.8)
(DPB)CoZn	387 (184.4)	542 (8.1)	559 (8.4)	578 (5.8)	
$(DPB)CoH_2$	384 (150.9)	516 (4.8)		563 (3.2)	635 (0.7)
$(DPA)H_4$	395 (190.5)	506 (14.1)	539 (5.1)	578 (6.0)	631 (3.3)
$(DPA)ZnH_2$	399 (196.6)	507 (7.0)	539 (10.5)	575 (11.6)	630 (1.3)
(DPA)CoZn	395 (167.6)	540 (11.5)	558 (9.5)	572 (10.5)	
$(DPA)CoH_2$	402 (177.3)	510 (8.7)	536 (6.2)	562 (7.8)	631 (1.3)
(EP-I)Zn[a]	402		532	568	
(DPB)Co(Me)Al(Me)[b]	389	560			
(DPB)Co(Me)Al(OMe)	385 (191.2)	549 (9.3)	560 (9.1)	581 (sh)	575 (sh)
(DPB)Co(Me)Al(OEt)	385 (186.8)	550 (8.9)	559 (9.0)	581 (sh)	575 (sh)
(DPB)Co(Me)Al(OBzl)	385 (183.2)	551 (8.5)	558 (8.9)	581 (sh)	575 (sh)
(DPA)Co(Me)Al(Me)[b]	395	557	591		
(DPA)Co(Me)Al(OMe)	392 (208.8)	542 (15.5)	560 (14.7)		
(DPA)Co(Me)Al(OEt)	391 (180.6)	543 (16.8)	561 (16.3)		
(DPA)Co(Me)Al(OBzl)	392 (196.7)	542 (14.8)	559 (14.7)		
(DPB)CoAl(OMe)	386 (182.9)	546 (7.7)	560 (8.1)	581 (sh)	
(DPB)CoAl(OEt)	386 (186.8)	548 (8.9)	559 (9.0)	582 (sh)	
(DPB)CoAl(OBzl)	386 (175.3)	547 (7.1)	560 (7.2)	582 (sh)	
(DPA)CoAl(OMe)	393 (195.9)	544 (13.7)	554 (13.6)	576 (sh)	
(DPA)CoAl(OEt)	393 (206.7)	544 (13.2)	553 (13.2)	575 (sh)	
(DPA)CoAl(OBzl)	393 (162.3)	544 (12.5)	554 (12.6)	576 (sh)	

[a] Taken from Edwards, L.; Dolphin, D. H.; Gouterman, M. *J. Mol. Spectrosc.* **1970**, *35*, 90–109. [b] Intermediate crude product.

complexes are summarized in Table IV. As shown in Figure 3, the UV–vis spectra are typical of the free-base, monometallic, and bimetallic porphyrin species. The free-base porphyrins exhibit four bands in the visible range, and their relative absorbance ratios indicate Phyllo-type spectra.[68] The Soret band and the visible bands are blue- and red-shifted, respectively, compared to the spectra of an analogous free-base monoporphyrin (5-(8-formyl-1-anthryl)-2,8,13,17-tetraethyl-3,7,12,18-tetramethylporphine ($(MPA)H_2$), λ_{max} (ϵ) nm (10^{-3} M^{-1} cm^{-1}): 404 (140), 502 (13.5), 535 (6.6), 569 (6.1), 624 (2.4)).[69] A Soret band broadening is also observed. These features are in good agreement with the cofacial geometry of the two porphyrin rings.[70] The DPB macrocycle spectrum for which the wavenumber shifts and band broadening are the most important indicates that the π-system interaction is largest, i.e., the interplanar distance is smallest.[71]

The monometallic diporphyrin spectra show similar changes for the Soret band compared to the analogous monoporphyrin spectra (see Table IV). However the wavelength shifts are smaller (for example, $\Delta\lambda((DPB)H_4-(MPA)H_2)$ = 25 nm, $\Delta\lambda((DPB)ZnH_2-(EP\text{-}I)Zn)$ = 14 nm for the Soret band), indicating that interaction between the two π-systems is different from that observed for the analogous free-base porphyrins. The data summarized in Table IV show that the Soret band wavelengths depend on the nature of the metal center. It is interesting to note that the X-ray studies in the Pacman series demonstrate the dependence on the slip angle on the nature of the metal ions (see crystallography section). Consequently, the wavelength shifts could arise from the coordination of one metal center and/or a different macrocycle conformation. In the visible range, the spectral shape results from the absorbance overlap of the free-base macrocycle and metalated porphyrin. The typical spectroscopic features of zinc and cobalt monoporphyrin are maintained, i.e., the zinc porphyrins exhibit a "regular" spectrum while the cobalt porphyrin spectrum is of the "hypso" type.[72]

The coordination of a second metal ion such as aluminum(III) does not induce a significant shift of the Soret band compared to the monocobalt porphyrin precursors. In contrast, the band shape in the visible range is typical. Each bimetallic complex exhibits three bands (see Table IV), whatever the nature of the metal ions; no cobalt oxidation state effect is observed. As previously described for the free-base and monometallic diporphyrins, the band shifts prove a clear interaction between the two π ring systems.

^{1}H NMR Spectrometry. The ^{1}H NMR data for the studied diamagnetic and paramagnetic complexes are summarized in Table V and Table VI, respectively. The ^{1}H NMR spectra for the $(DPB)H_4$ and $(DPA)H_4$ free-base porphyrins have been previously reported.[23-25] The NH proton resonances for the free bases and the monozinc diporphyrin complexes ($(DPB)H_4$, $(DPA)H_4$, $(DPB)ZnH_2$, and $(DPA)ZnH_2$) give two distinct signals in C_6D_6; the chemical shift differences between these two signals ($\Delta\delta$ (ppm)) decrease according to the following sequence: $\Delta\delta((DPA)H_4) > \Delta\delta((DPB)H_4) > \Delta\delta((DPB)ZnH_2) > \Delta\delta((DPA)ZnH_2)$ (see Table V). These results indicate the disappearance of the C_2 axis of symmetry bisecting the bridging group (anthracenyl and biphenylenyl groups).[35] The strongest porphyrin skeletal distortion is observed for the $(DPA)H_4$ free-base porphyrin for which the interplanar distance is the largest, as shown by the UV–vis data as well as by the fact that the NH proton shielding for this macrocycle is the lowest.

When a cobalt(II) ion is coordinated to one of the two porphyrin rings, the NH proton resonances on the other porphyrin appear at high field ($(DPA)CoH_2$, δ(NH) = −20.00 and −20.44 ppm; $(DPB)CoH_2$, δ(NH) = −37.13 and −46.03 ppm in C_6D_6 at 294 K). The high-field resonances of the ^{1}H NMR spectra of $(DPA)H_4$, $(DPB)H_4$, $(DPB)ZnH_2$, $(DPA)ZnH_2$, $(DPA)CoH_2$, and $(DPB)CoH_2$ recorded in C_6D_6 at 294 K are presented in Figure 4. The cobalt porphyrin spectra are typical of a coordinated low-spin cobalt(II) ion.[73] The electronic ground state of low spin Co(II) is $^2A_1(d_{z^2})$. Thus the ^{1}H NMR spectra are dominated by the effect of the unpaired electron on the cobalt(II) ion which induces large isotropic shifts and broadening of the proton resonances.[74] Compared to the resonances of analogous diamagnetic complexes, the large chemical shift differences for the NH protons of the cobalt(II) derivatives can be attributed to the paramagnetic shift which results from dipolar and Fermi

(68) Smith, K. M. In *Porphyrins and Metalloporphyrins*; Smith, K. M., Ed.; Elsevier Scientific: Amsterdam, 1975; pp 3–28.
(69) Abdalmuhdi, I.; Chang, C. K. *J. Org. Chem.* **1985**, *50*, 411–413.
(70) Collman, J. P.; Elliot, C. M.; Halbert, T. R.; Tovrog, B. S. *Proc. Natl. Acad. Sci. USA* **1977**, *74*, 18–22.
(71) Chang, C. K. *J. Heterocycl. Chem.* **1977**, *14*, 1285–1288.
(72) Gouterman, M. In *The Porphyrins*; Dolphin, D., Ed.; Academic: New York, 1978; pp 1–165.
(73) La Mar, G. N.; Walker, F. A. In *The Porphyrins*; Dolphin, D., Ed.; Academic: New York, 1978; pp 61–157.
(74) La Mar, G. N.; Walker, F. A. *J. Am. Chem. Soc.* **1973**, *95*, 1790–1796.

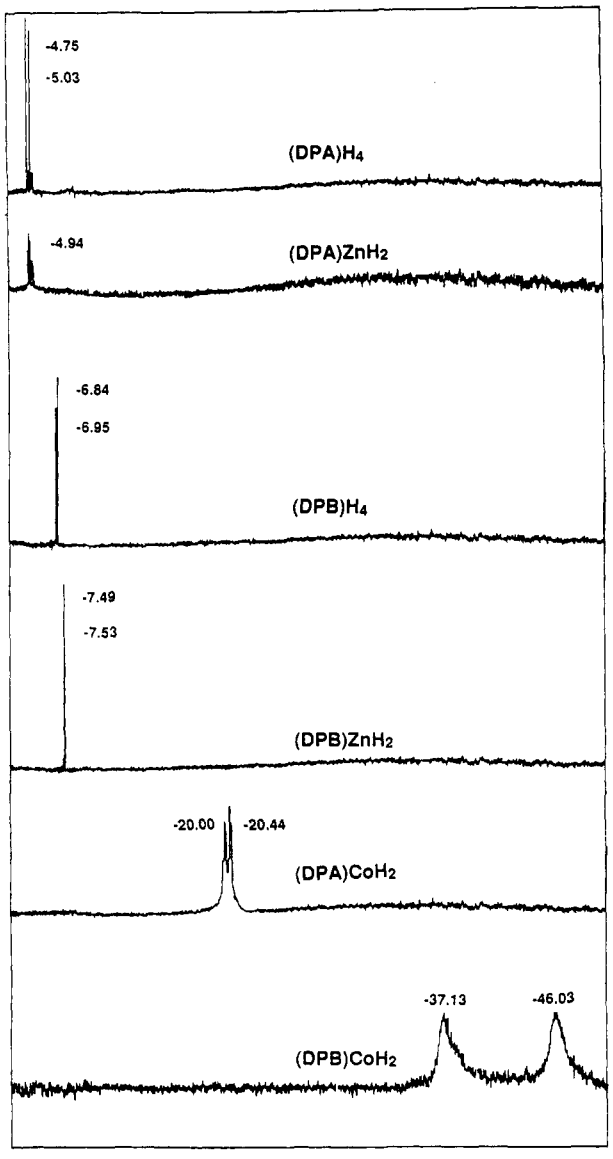

Figure 4. High-field regions of the ^1H NMR spectra of $(DPA)H_4$, $(DPB)H_4$, $(DPB)ZnH_2$, $(DPA)ZnH_2$, $(DPA)CoH_2$, and $(DPB)CoH_2$ recorded in C_6D_6 at 294 K.

interactions. The presence of an unpaired electron in a d_{z^2} orbital may induce a major contribution to the dipolar interaction. The data summarized in Table VI agree well with this hypothesis since the main contribution arises from a through-space interaction of the unpaired electron with protons. The strongest interaction is normally observed in the DPB series for which the interplanar porphyrin distance is the shortest.

Surprisingly, the resonances of the H_{20} and H_{10} meso protons appear at much lower field than that of the H_{15} meso protons ($\Delta\delta \approx 7$ ppm). The ring current of the close bridging group could possibly explain such a result. As described below, the same characteristics are observed when an aluminum(III) ion is coordinated to the second porphyrin macrocycle.

The ^1H NMR data for the diamagnetic cobalt(III)–aluminum(III) complexes are summarized in Table V. As expected, the porphyrin ring current induces a large shielding for the protons of the σ-bonded group (Table VII, Figure 5).[65,75] The axial methyl protons for the (DPB)Co(Me)Al(OR) and (DPA)Co(Me)Al(OR) complexes are observed at −6.17 and −5.28 ppm, respectively (Table VII), and no effect on the axial alkoxide ligand bonded to the aluminum ion is observed. The data for the DPA complex are close to those observed for the (OEP)Co(Me) derivative for which the axial methyl proton resonance appears at −5.20 ppm

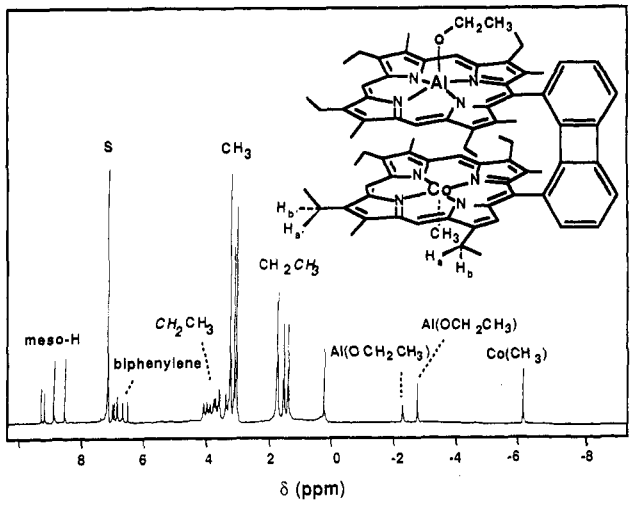

Figure 5. ^1H NMR spectra of $(DPB)Co(CH_3)Al(OCH_2CH_3)$ recorded in C_6D_6 at 294 K.

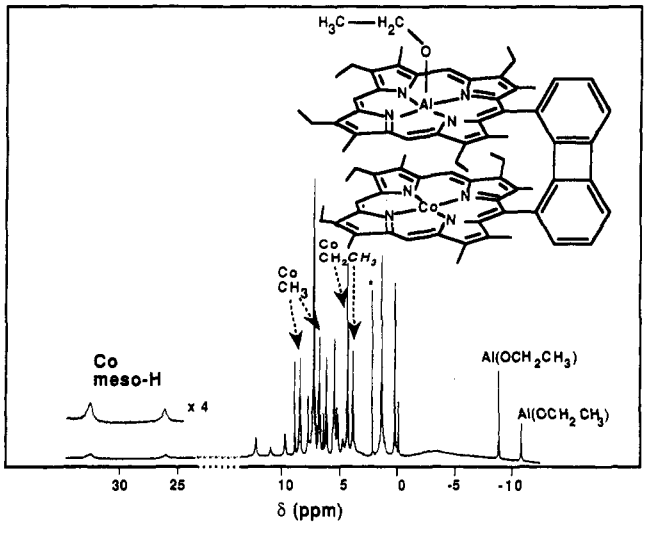

Figure 6. ^1H NMR spectra of $(DPB)CoAl(OCH_2CH_3)$ recorded in C_6D_6 at 294 K.

in the same solvent. As expected, the DPB complexes give the most significant ring interaction. The axial alkoxide–aluminum proton chemical shifts follow the same trend. Indeed the resonances are at lower field than those reported for analogous aluminum monoporphyrin complexes,[76] and the largest difference occurs for the DPB series (Table VII). The chemical shifts for the axial ligands of the two porphyrin moieties are in agreement with those previously described for monocobalt or monoaluminum porphyrins. This observation leads us to postulate that the ligands are located outside of the diporphyrin cavity since the large shielding normally observed inside the cavity does not occur.[35]

As already described for the monometallic compounds, the cobalt(II) paramagnetism induces significant chemical shifts and signal broadening in the ^1H NMR spectra of cobalt(II)–aluminum(III) complexes. This is well demonstrated by the paramagnetic effect of the low-spin cobalt(II) ion on the alkoxide ligands coordinated to the aluminum(III) metal (Figure 6). The ^1H NMR data for the (DP)CoAl(OR) complexes summarized in Table VIII show that the axial proton signals are observed at higher field compared to those for the $(DP)Co(R_1)Al(OR_2)$ precursors. The larger chemical shift difference (>8 ppm) occurs for the OCH_3 or OCH_2 sites. This difference normally decreases when the distance from the paramagnetic center increases (Table VIII). For the same axial ligand the shielding is lower in the DPA

(75) Brothers, P. J.; Collman, J. P. *Acc. Chem. Res.* **1986**, *19*, 209–215.

(76) Asano, S.; Aida, T.; Inoue, S. *Macromolecules* **1985**, *18*, 2057–2061.

Table V. ^{1}H NMR Data for the (DPB)H_4 and (DPA)H_4 Free-Base Porphyrins and Their Corresponding Diamagnetic Complexes[a]

compound	unit	δ (ppm) (m/*i*)[a]																							
		H_{meso}		H_a		H_b		CH_2CH_3		CH_3				$H_{biphenyl}$ or $H_{anthracenyl}$						$H_{axial\ ligand}$				NH	
(DPB)H_4		9.19 (s/2)	8.64 (s/4)	4.16 (m/4)	3.90 (m/4)	3.79 (m/4)	3.56 (m/4)	1.75 (t/12)	1.48 (t/12)	3.16 (s/12)	3.14 (s/12)			6.97 (d/2)	6.76 (t/2)	6.70 (d/2)								−6.84 (s/2)	−6.95 (s/2)
(DPB)ZnH_2	(P)H_2	9.32 (s/1)	8.85 (s/2)	4.11 (m/2)	3.97 (m/2)	3.68 (m/2)	3.56 (m/2)	1.59 (t/6)	1.53 (t/6)															−7.49 (s/1)	−7.53 (s/1)
	(P)Zn	8.81 (s/1)	8.74 (s/2)	4.19 (m/2)	3.84 (m/2)	4.11 (m/2)	3.73 (m/2)	1.77 (t/6)	1.64 (t/6)	3.28 (s/6)	3.27 (s/6)	3.23 (s/6)	3.06 (s/6)	7.00 (d/1)	6.98 (d/1)	6.90 (d/1)	6.84 (t/1)	6.60 (t/1)	6.23 (d/1)						
(DPA)H_4		9.48 (s/2)	8.80 (s/4)	4.09 (m/4)	3.35 (m/4)	3.82 (m/4)	3.23 (m/4)	1.73 (t/12)	1.28 (t/12)	3.01 (s/12)	1.99 (s/12)			8.67 (s/1)	8.28 (d/2)	7.49 (m/4)	7.42 (s/1)							−4.75 (s/2)	−5.03 (s/2)
(DPA)ZnH_2	(P)H_2	9.47 (s/1)	9.02 (s/2)	4.03 (m/2)	3.57 (m/2)	3.82 (m/2)	3.37 (m/2)	1.71 (t/6)	1.40 (t/6)															−4.94 (M/2)	
	(P)Zn	9.37 (s/1)	9.14 (s/2)	3.93 (m/2)	3.68 (m/2)	3.74 (m/2)	3.48 (m/2)	1.65 (t.6)	1.46 (t/6)	3.13 (s/6)	3.06 (s/6)	2.10 (s/6)	2.06 (s/6)	8.73 (s/1)	8.32 (dd/2)	7.56–7.43 (m/5)									
(DPB)Zn_2		9.14 (s/2)	8.79 (s/4)	4.19 (m/4)	3.81 (m/4)	4.03 (m/4)	3.62 (m/4)	1.73 (t/12)	1.52 (t/12)	3.25 (s/12)	3.19 (s/12)			6.96 (d/2)	6.73 (t/2)	6.68 (d/2)									
(DPA)Zn_2		9.44 (s/2)	9.20 (s/4)	3.85 (m/4)	3.66 (m/4)	3.73 (m/4)	3.56 (m/4)	1.61 (t/12)	1.50 (t/12)	3.04 (s/12)	2.19 (s/12)			8.81 (s/1)	8.38 (d/2)	7.94 (m/4)	7.53 (s/1)								
(DPB)Co(Et)-Al(OMe)	(P)Co(Et)	9.24 (s/2)	8.50 (s/4)	4.01 (m/4)	3.58 (m/4)	3.71 (m/4)	3.35 (m/4)	1.73 (t/12)	1.38 (t/12)											−5.34 (q/2)	−6.35 (t/3)				
	(P)Al(OMe)	9.30 (s/2)	8.87 (s/4)	4.09 (m/4)	3.75 (m/4)	3.86 (m/4)	3.58 (m/4)	1.74 (t/12)	1.49 (t/12)	3.26 (s/6)	3.11 (s/6)	3.06 (s/6)	3.05 (s/6)							−2.23 (s/3)					
(DPB)Co-(Me)-Al(OMe)	(P)Co(Me)	9.17 (s/1)	8.53 (s/2)	3.96 (m/2)	3.58 (m/2)	3.69 (m/2)	3.36 (m/2)	1.71 (t/6)	1.37 (t/6)											−6.16 (s/3)					
	(P)Al(OMe)	9.31 (s/1)	8.88 (s/2)	4.04 (m/2)	3.75 (m/2)	3.86 (m/2)	3.58 (m/2)	1.73 (t/6)	1.50 (t/6)	3.25 (s/6)	3.13 (s/6)	3.06 (s/6)	3.05 (s/6)	6.97 (d/1)	6.92 (d/1)	6.78 (m/2)	6.64 (t/1)	6.49 (d/1)							
(DPB)Co-(Me)-Al(OEt)	(P)Co(Me)	9.18 (s/1)	8.53 (s/2)	3.95 (m/2)	3.58 (m/2)	3.69 (m/2)	3.35 (m/2)	1.71 (t/6)	1.37 (t/6)											−2.23 (s/3)					
	(P)Al(OEt)	9.28 (s/1)	8.87 (s/2)	4.06 (m/2)	3.74 (m/2)	3.86 (m/2)	3.58 (m/2)	1.74 (t/6)	1.51 (t/6)	3.25 (s/6)	3.11 (s/6)	3.06 (s/6)	3.04 (s/6)	6.97 (d/1)	6.91 (d/1)	6.81 (m/2)	6.64 (t/1)	6.47 (d/1)		−6.17 (s/3)					
(DPB)Co-(Me)-Al(OBzl)	(P)Co(Me)	9.14 (s/1)	8.53 (s/2)	*b*	3.60 (m/2)	3.68 (m/2)	3.36 (m/2)	1.70 (t/6)	1.37 (t/6)											−2.28 (q/2)	−2.76 (t/3)				
	(P)Al(OBzl)	9.28 (s/1)	8.87 (s/2)	4.06 (m/2)	3.74 (m/2)	3.86 (m/2)	3.58 (m/2)	1.74 (t/6)	1.51 (t/6)	3.22 (s/6)	3.12 (s/6)	3.05 (s/6)	3.04 (s/6)	6.81 (t/1)	6.72 (d/1)	6.63 (t/1)	6.47 (t/1)	*b*		−6.18 (s/3)					
(DPA)Co-(Me)-Al(OMe)	(P)Co(Me)	9.58 (s/1)	8.55 (s/2)	3.88 (m/2)	3.30 (m/2)	3.43 (m/2)	2.84 (m/2)	1.32 (t/6)	0.90 (t/6)											−1.32[c] (s/2)	3.49[c] (d/2)	5.98[c] (t/2)	6.23[c] (t/1)		
	(P)Al(OMe)	9.72 (s/1)	8.66 (s/2)	3.97 (m/2)	3.70 (m/2)	3.74 (m/2)	3.09 (m/2)	1.76 (t/6)	1.16 (t/6)	2.73 (s/6)	2.68 (s/6)	2.03 (s/6)	1.85 (s/6)	8.92 (s/1)	8.21 (m/2)	7.77 (s/1)	7.52 (dd/2)	7.39 (dd/2)		−5.28 (s/3)					
(DPA)Co-(Me)-Al(OEt)	(P)Co(Me)	9.58 (s/1)	8.55 (s/2)	3.88 (m/2)	3.23 (m/2)	3.32 (m/2)	2.85 (m/2)	1.33 (t/6)	0.90 (t/6)											−1.59 (s/3)					
	(P)Al(OEt)	9.75 (s/1)	8.67 (s/2)	3.97 (m/2)	3.69 (m/2)	3.75 (m/2)	3.09 (m/2)	1.77 (t/6)	1.16 (t/6)	2.73 (s/6)	2.67 (s/6)	2.04 (s/6)	1.85 (s/6)	8.92 (s/1)	8.21 (m/2)	7.80 (s/1)	7.54 (dd/2)	7.39 (dd/2)		−5.28 (s/3)					
(DPA)Co-(Me)-Al(OBzl)	(P)Co(Me)	9.57 (s/1)	8.51 (s/2)	3.87 (m/2)	3.10 (m/2)	3.44 (m/2)	2.84 (m/2)	1.34 (t/6)	0.90 (t/6)											−1.60 (q/2)	−2.27 (t/3)				
	(P)Al(OBzl)	9.69 (s/1)	8.66 (s/2)	3.95 (m/2)	3.67 (m/2)	3.71 (m/2)	3.04 (m/2)	1.75 (t/6)	1.16 (t/6)	2.73 (s/6)	2.66 (s/6)	2.01 (s/6)	1.85 (s/6)	8.93 (s/1)	8.21 (m/2)	7.73 (s/1)	7.53 (dd/2)	7.38 (dd/2)		−5.29 (s/3)					
																				−0.62[c] (s/2)	3.44[c] (d/2)	6.09[c] (t/2)	6.29[c] (t/1)		

[a] Spectra were recorded in C_6D_6 at 21 °C with $SiMe_4$ as internal reference. Chemical shifts downfield from $SiMe_4$ are defined as positive. Key: s = singlet; d = doublet; t = triplet; m = multiplet; M = broad signal. [b] The signal cannot be observed due to the benzyl alcohol resonances. [c] Assignments are as follows across column: $-OCH_2$, *o*-H, *m*-H, *p*-H.

Table VI. Proton Chemical Shifts of the Investigated Cobalt(II) Pacman Porphyrins and Their Separation into Dipolar and Contact Contributions (C_6D_6, 294 K)

compound	proton type	δ (ppm)		$(\Delta H/H)^{iso}$ (ppm)[a]		geometric factor ($Å^{-3}$)[b]		$(\Delta H/H)_{dip}$ (ppm)		$(\Delta H/H)_{con}$ (ppm)	
(DPB)CoZn[c]	α-CH_3	7.85	5.90	4.60	2.71			5.2		−0.6	−2.5
	β-CH_3	4.44	4.07	2.71	2.55			3.2		−0.5	−0.6
	meso-H	31.14	24.90	22.35	15.76			15		7.3	0.8
(DPA)CoZn[c]	α-CH_3	7.62	6.10	4.58	3.91			5.2		−0.6	−1.3
	β-CH_3	4.98	4.76	3.28	3.26			3.2		0.1	0.1
	meso-H	30.92	24.93	21.72	15.49			15		6.7	0.5
(DPB)CoH_2[c]	α-CH_3	7.86	6.22	4.61	3.03			5.2		−0.6	−2.2
	β-CH_3	4.28	3.97	2.55	2.45			3.2		−0.6	−0.7
	meso-H	31.64	24.75	22.85	15.61			15		7.8	0.6
(DPA)CoH_2[c]	α-CH_3	8.0	6.25	4.96	4.06			5.2		−0.2	−1.1
	β-CH_3	5.13	5.13	3.52	3.63			3.2		0.3	0.4
	meso-H	31.82	25.30	22.62	15.86			15		7.6	0.9
(EP-I)Co[c]	α-CH_3			4.73				5.2		−0.5	
	β-CH_3			3.92				3.2		0.7	
	meso-H			17.57				15		2.6	
(DPB)CoAl(OMe)	α-CH_3	8.38	6.07	5.13	2.88	−0.0044	−0.0040	6.09	5.5	−1.0	−2.7
	β-CH_3	4.22	3.80	2.49	2.28	−0.0019	−0.0028	2.63	3.88	−0.1	−1.6
	meso-H	32.71	26.09	23.92	16.95	−0.0113	−0.0104	15.7	14.4	8.2	2.5
(DPB)CoAl(OEt)	α-CH_3	8.35	6.08	5.10	2.89	−0.0044	−0.0040	6.09	5.5	−1.0	−2.6
	β-CH_3	4.23	3.77	2.50	2.25	−0.0019	−0.0028	2.63	3.88	−0.1	−1.6
	meso-H	32.64	26.09	23.85	16.95	−0.0113	−0.0104	15.7	14.4	8.2	2.5
	$AlOCH_2CH_3$[d]	−10.79		−8.51		+0.0050		−6.94		−1.57	
	$AlOCH_2CH_3$[d]	−8.84		−6.08		+0.0039		−5.44		−0.64	
(DPB)CoAl(OBzl)	α-CH_3	8.37	6.07	5.12	2.88	−0.0044	−0.0040	6.09	5.5	−1.0	−2.6
	β-CH_3	4.19	3.79	2.46	2.27	−0.0019	−0.0028	2.63	3.88	−0.2	−1.6
	meso-H	32.67	26.08	23.88	16.94	−0.0113	−0.0104	15.7	14.4	8.2	2.5
(DPA)CoAl(OMe)[c]	α-CH_3	8.05	6.09	5.01	3.90			5.2		−0.2	−1.3
	β-CH_3	5.36		3.75				3.2		0.6	
	meso-H	31.97	26.33	22.53	17.13			15		7.5	2.1
(DPA)CoAl(OEt)[c]	α-CH_3	8.02	6.08	4.98	3.89			5.2		−0.2	−1.3
	β-CH_3	5.35		3.74				3.2		0.5	
	meso-H	31.90	26.30	22.46	17.10			15		7.5	2.1
(DPA)CoAl(OBzl)[c]	α-CH_3	8.04	6.09	5.00	3.90			5.2		−0.2	−1.3
	β-CH_3	5.35		3.74				3.2		0.5	
	meso-H	31.97	26.38	22.53	17.18			15		7.5	2.2

[a] Referenced against the diamagnetic (DPB)Zn_2 and (DPA)Zn_2 complexes in C_6D_6. [b] Axial geometric factor, $\langle(3\cos^2\theta - 1)/r^3\rangle_{av}$. [c] Reference 73. [d] Referenced against the diamagnetic (DPB)Co(Me)Al(OEt) complex in C_6D_6.

Table VII. Axial Ligand Chemical Shifts for the (DP)Co(Me)Al(OR) Complexes (C_6D_6, 294 K)

compound	axial ligand	proton type	δ (ppm) DPA	δ (ppm) DPB
(DP)Co(Me)Al(OMe)	$Al(OCH_3)$	CH_3	−1.59	−2.23
	$Co(CH_3)$	CH_3	−5.28	−6.16
(DP)Co(Me)Al(OEt)	$Al(OCH_2CH_3)$	CH_2	−1.60	−2.28
		CH_3	−2.27	−2.76
	$Co(CH_3)$	CH_3	−5.28	−6.17
(DP)Co(Me)Al(OBzl)	$Al(OCH_2C_6H_5)$	CH_2	−0.62	−1.32
		o-H	3.44	3.49
		m-H	6.09	5.98
		p-H	6.29	6.23
	$Co(CH_3)$	CH_3	−5.29	−6.18

series ($\Delta\delta \approx 5.5$ ppm for the OCH_3 or OCH_2 protons, see Table VIII).

The contact and dipolar contributions to isotropic shifts have been calculated according to the empirical method of La Mar and Walker[73] (see Table VI). The geometric factors for different proton sites of (DPB)CoAl(OCH_2CH_3) have been determined from the X-ray structural data, and the geometric factors have been postulated to be identical for the same porphyrin proton sites in the other Pacman cobalt–aluminum complexes. As expected, the main contribution to isotropic shifts arises from the pseudo-contact interaction. In agreement with the data observed for the monocobalt complexes, the large contact shift for the H_{20} and H_{10} meso proton sites is possibly the result of the close proximity of the bridging group. For the axial ethoxide group the largest

Table VIII. Alkoxide Axial Ligand Chemical Shifts for the (DP)Co(Me)Al(OR) and (DP)CoAl(OR) Complexes (C_6D_6, 294 K)

axial ligand	proton type	δ (ppm) (DPB)Co(CH_3)Al(OR)	δ (ppm) (DPB)CoAl(OR)	$\Delta\delta$[a] (ppm)
CH_3	CH_3	−2.22	−10.39	8.17
CH_2CH_3	CH_2	−2.28	−10.79	8.51
	CH_3	−2.76	−8.84	6.08
$CH_2C_6H_5$	CH_2	−1.31	−9.75	8.44
	o-H	3.49	2.11	1.38
	m-H	5.98	3.29	2.69
	p-H	6.23	4.07	2.16
		(DPA)Co(CH_3)Al(OR)	(DPA)CoAl(OR)	
CH_3	CH_3	−1.59	−6.67	5.08
CH_2CH_3	CH_2	−1.60	−6.97	5.37
	CH_3	−2.27	−6.36	4.09
$CH_2C_6H_5$	CH_2	−0.62	−6.08	5.46
	o-H	3.44	2.74	0.70
	m-H	6.09	3.86	2.23
	p-H	6.29	4.60	1.69

[a] $\Delta\delta = |\delta_{para} - \delta_{dia}|$.

Table IX. ESR Data for the Cobalt(II) Complexes under Inert Atmosphere (Toluene, 100 K)

compound	$g_\parallel$	$g_\perp$	$g_\parallel^2 - g_\perp^2$	$10^{-4}\lvert A_\parallel\rvert$ (cm^{-1})	$10^{-4}\lvert A_\perp\rvert$ (cm^{-1})
(DPB)CoAl(OEt)	1.91	3.32	−7.37	190	369
(*p*-CH_3TPP)Co[a,b]	1.825	3.257	−7.28	179	359
(DPB)CoAl(OMe)	1.91	3.28	−7.11	192	355
(DPB)CoAl(OBzl)	1.91	3.27	−7.04	190	353
(DPB)CoZn	1.98	3.21	−6.38	204	327
(DPB)CoH_2	2.00	3.18	−6.11	198	315
(DPA)CoAl(OMe)	2.02	3.11	−5.59	163	219
(DPA)CoAl(OEt)	2.02	3.10	−5.53	159	205
(DPA)CoAl(OBzl)	2.02	3.10	−5.53	161	207
(*p*-CH_3TPP)Co[a]	1.966	~2.97	−4.96	138	~272
(OEP)Co[a]	1.946	2.927	−4.78	136	246
(DPA)CoH_2	2.03	2.97	−4.70	167	261
(DPA)CoZn	2.01	2.95	−4.66	168	250

[a] From Walker, F. A. *J. Magn. Reson.* **1974**, *15*, 201–218. [b] In polycrystalline state.

dipolar shift (−6.94 ppm) is observed for the CH_2 site. The difference between the two proton site resonances fits well the distance changes from the paramagnetic center: $(\Delta H/H)_{CH_2}^{iso}/(\Delta H/H)_{CH_3}^{iso} = 1.4$ and $r_{CH_2}^{-3}/r_{CH_3}^{-3} = 1.3$. The large paramagnetic chemical shifts for the protons on axial ligands bound to aluminum as well as those for pyrrolic NHs of the monocobalt DPA and DPB complexes (see previous paragraph) could be interpreted by a simple dipole interaction ($\Delta\delta = \mu(1 - 3\cos^2\theta)/r^3$, where $\Delta\delta$ is the change in chemical shift of a nucleus, μ is the paramagnetic moment, and $(1 - 3\cos^2\theta)/r^3$ is the corresponding geometric term).[77]

The Curie plot of different proton sites of (DPB)CoH_2 and (DPB)CoAl(OCH_3) confirms that the paramagnetic shifts are mainly due to a dipolar interaction (Figure 7). The NH and axial methoxide proton chemical shifts for the (DPB)CoH_2 and (DPB)CoAl(OCH_3) complexes exhibit the same behavior. The isotropic shifts of these proton sites decrease with the temperature. In contrast, the other porphyrin proton isotropic shifts increase when the temperature decreases. The same characteristics were reported for NMR data of a series of benzenoid capped porphyrins.[78] The deviation from Curie's law may result from magnetic anisotropy changes with the temperature.[74]

ESR Spectroscopy. ESR data of the cobalt(II) complexes recorded under an inert atmosphere in toluene at 100 K are summarized in Table IX. Each complex exhibits an ESR spectrum typical of a low-spin d^7 cobalt(II) complex. The $g_\parallel$ and $g_\perp$ values are in the range of 1.91–2.03 and 2.95–3.32, respectively. The $g_\parallel^2 - g_\perp^2$ difference reflects the magnetic anisotropy for a given porphyrin complex. It is clear that the DPB series magnetic anisotropy is close to that observed for (*p*-CH_3TPP)Co in solid state. In contrast, the DPA complex ESR data can be compared to those of the monoporphyrin cobalt derivative in a toluene glass. The large anisotropy in the DPB series is attributable to an intramolecular macrocycle interaction, as already detailed in the NMR section. Furthermore, the magnetic anisotropy calculated from the NMR data ($g_\parallel^2 - g_\perp^2 = -8.2 \pm 0.1$) is close to the ESR value determined at low temperature. In contrast to the data observed for the cobalt monoporphyrin complexes, the DPB complex magnetic anisotropy does not depend on the nature of the solvent. Their characteristics are similar to those of unsolvated polycrystalline cobalt monoporphyrin complexes where intermolecular interactions have been invoked.[79] Such interaction may be weak in the DPA series as for a monoporphyrin, and their behavior can be compared to that of the (*p*-CH_3TPP)Co complex in toluene.

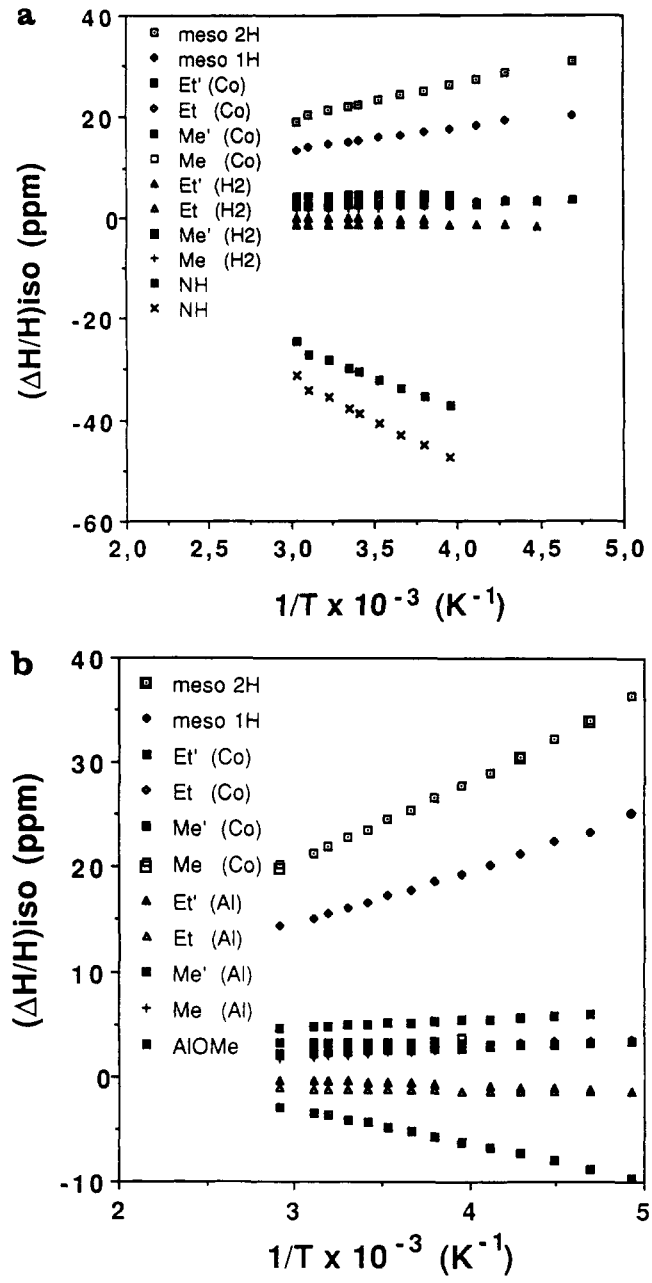

Figure 7. Curie plot for the paramagnetic shifts in the ^1H NMR spectra of (a) (DPB)CoH_2 and (b) (DPB)CoAl(OCH_3) in toluene-d_8.

The physiochemical characterization of the oxygenated species and the use of the title compounds as catalyst for oxygen reduction are under way.

Acknowledgment. Support from C.N.R.S., the National Science Foundation, and the National Institutes of Health is gratefully acknowledged.

Supplementary Material Available: Tables of anisotropic thermal motion parameters, bond distances and angles, positional parameters for hydrogen atoms, least-squares planes, positional parameters and estimated standard deviations, and an ORTEP drawing of (DPB)CoAl(OEt) (13 pages); a list of structure factors (31 pages). Ordering information is given on any current masthead page.

(77) Abraham, R. J.; Marsden, I.; Xiujing, L. *Magn. Reson. Chem.* **1990**, *28*, 1051–1057.
(78) Clayden, N. J.; Moore, G. R.; Williams, R. J. P.; Baldwin, J. E.; Crossley, M. J. *J. Chem. Soc., Perkin Trans. II* **1983**, 1863–1868.
(79) Maillard, P.; Giannotti, C. *J. Organomet. Chem.* **1979**, *181*, C11–C13.